Diagnostic Imaging

Nuclear Medicine

SECOND EDITION

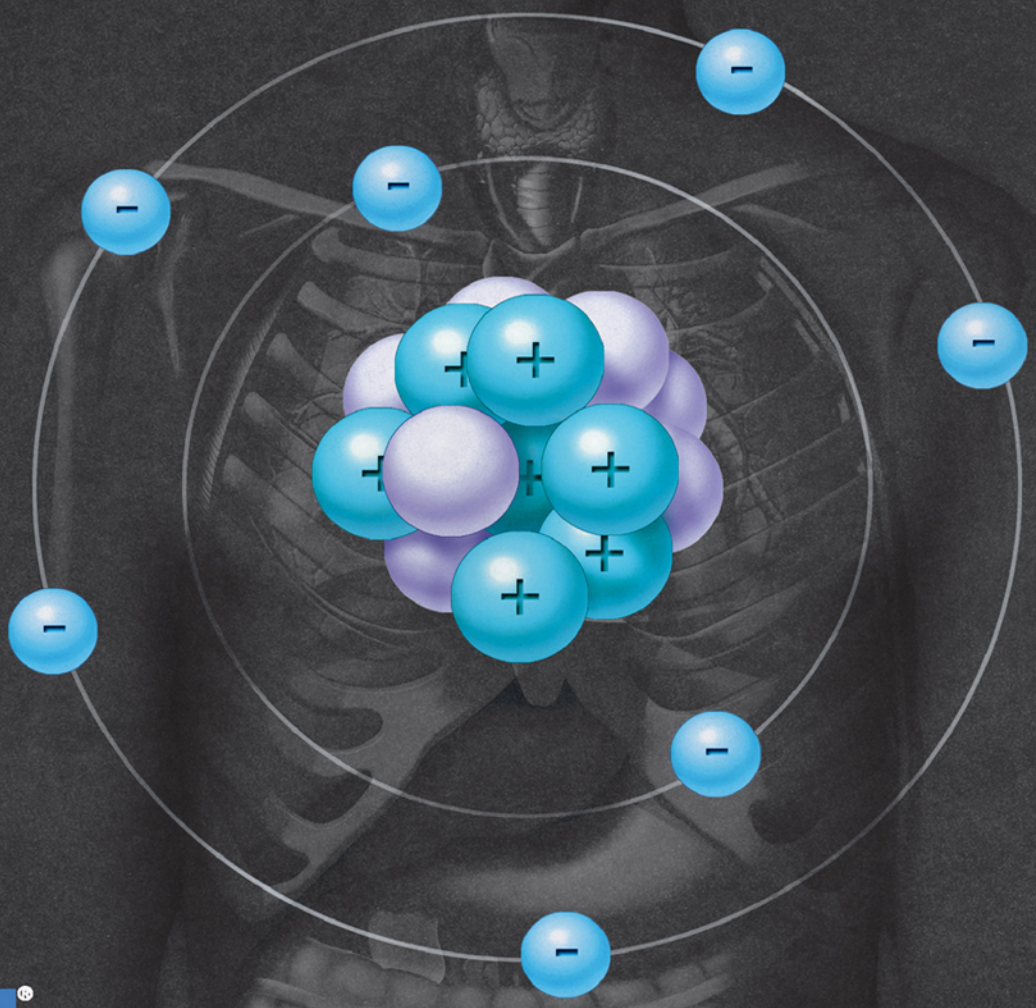

Bennett | Oza

TROUT • MINTZ

AMIRSYS®

ELSEVIER

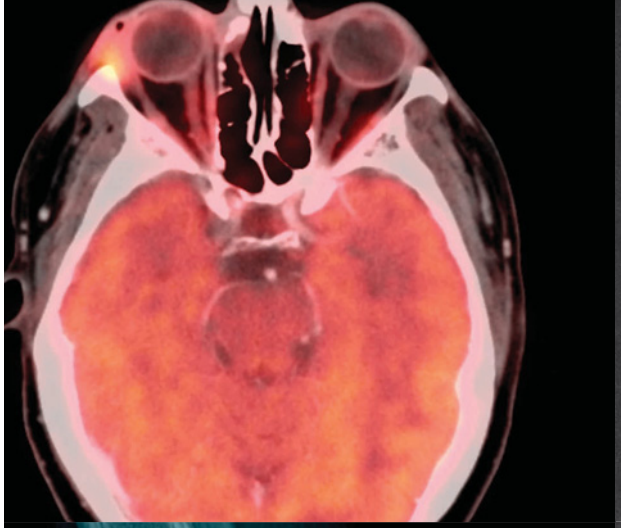

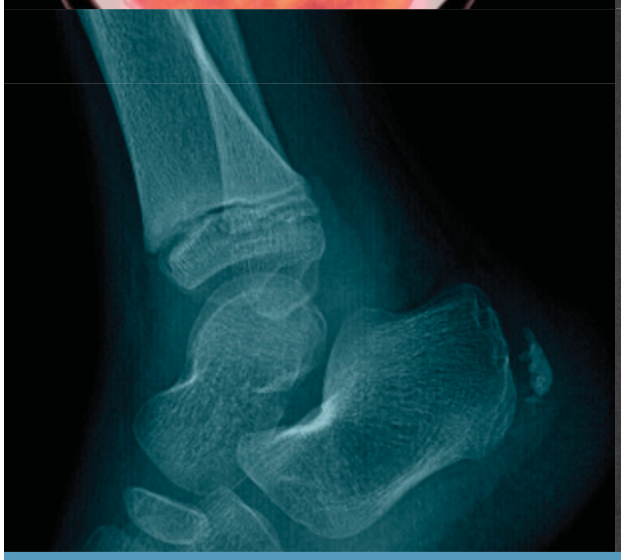

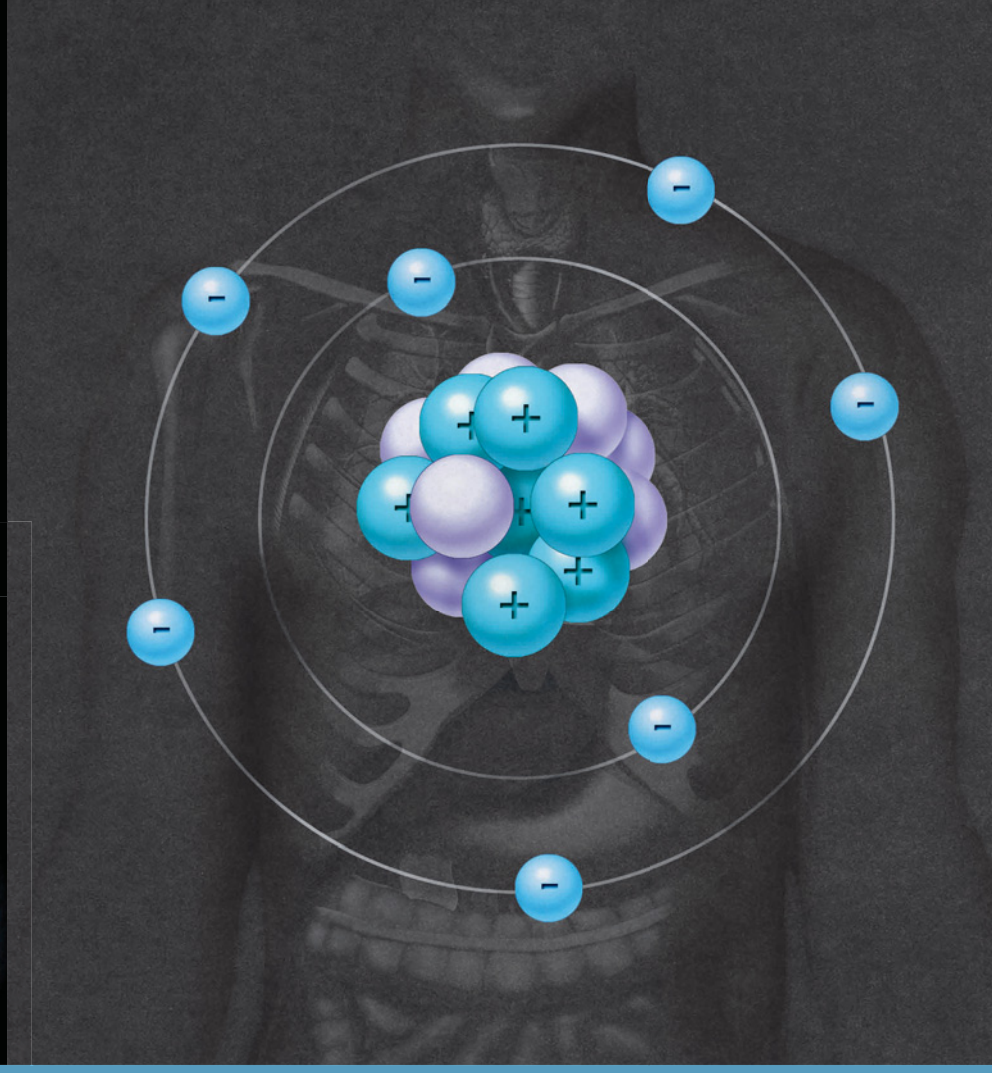

Diagnostic Imaging

Nuclear Medicine

SECOND EDITION

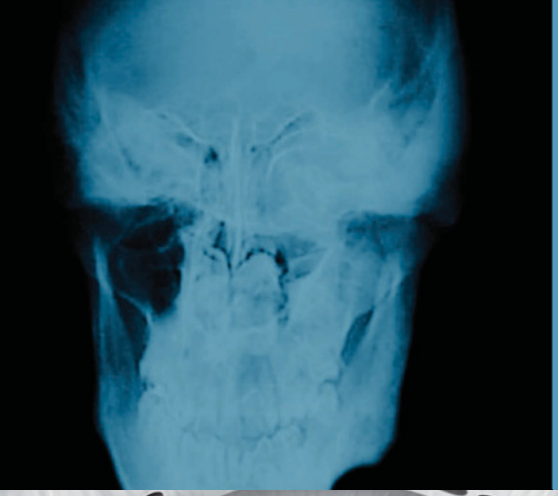

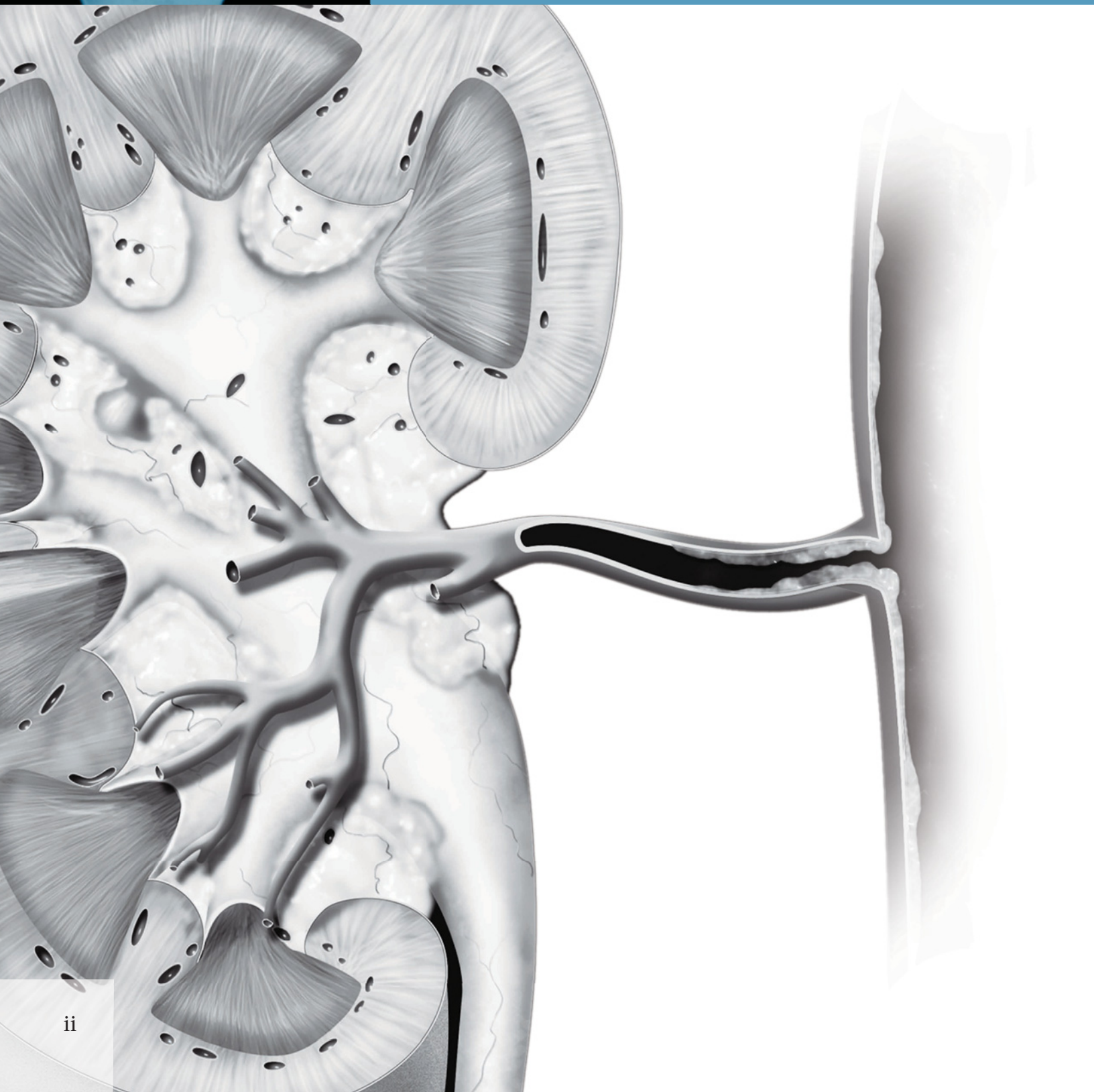

Diagnostic Imaging

Nuclear Medicine

SECOND EDITION

Paige Bennett, MD

Associate Professor
Nuclear Medicine and Molecular Imaging
Department of Radiology
Wake Forest School of Medicine
Winston-Salem, North Carolina

Umesh D. Oza, MD

Diagnostic Radiology Residency Program Director
Baylor University Medical Center at Dallas
Clinical Associate Professor
Texas A&M Health Science Center College of Medicine
College Station, Texas

Andrew T. Trout, MD

Assistant Professor of Radiology and Pediatrics
Department of Radiology
Cincinnati Children's Hospital Medical Center
Cincinnati, Ohio

Akiva Mintz, MD, PhD, MHA, CFA

Vice Chair of Finance, Department of Radiology
Section Head, Nuclear Medicine and Molecular Imaging
Department of Radiology and Neurosurgery
Leader, Translational Imaging Program
Assistant Director, Wake Forest Clinical & Translational Science Institute (CTSI)
Wake Forest School of Medicine
Winston-Salem, North Carolina

ELSEVIER

1600 John F. Kennedy Blvd.
Ste 1800
Philadelphia, PA 19103-2899

DIAGNOSTIC IMAGING: NUCLEAR MEDICINE, SECOND EDITION ISBN: **978-0-323-37753-9**

Notices

Knowledge and best practice in this field are constantly changing. As new research and experience broaden our understanding, changes in research methods, professional practices, or medical treatment may become necessary.

Practitioners and researchers must always rely on their own experience and knowledge in evaluating and using any information, methods, compounds, or experiments described herein. In using such information or methods they should be mindful of their own safety and the safety of others, including parties for whom they have a professional responsibility.

With respect to any drug or pharmaceutical products identified, readers are advised to check the most current information provided (i) on procedures featured or (ii) by the manufacturer of each product to be administered, to verify the recommended dose or formula, the method and duration of administration, and contraindications. It is the responsibility of practitioners, relying on their own experience and knowledge of their patients, to make diagnoses, to determine dosages and the best treatment for each individual patient, and to take all appropriate safety precautions.

To the fullest extent of the law, neither the Publisher nor the authors, contributors, or editors, assume any liability for any injury and/or damage to persons or property as a matter of products liability, negligence or otherwise, or from any use or operation of any methods, products, instructions, or ideas contained in the material herein.

Publisher Cataloging-in-Publication Data

Diagnostic imaging. Nuclear medicine / [edited by] Paige Bennett and Umesh D. Oza.
2nd edition.
pages ; cm
Nuclear medicine
Includes bibliographical references and index.
ISBN 978-0-323-37753-9 (hardback)
1. Diagnostic imaging--Handbooks, manuals, etc. 2. Nuclear medicine--Handbooks, manuals, etc.
I. Bennett, Paige. II. Oza, Umesh D. III. Title: Nuclear medicine.
[DNLM: 1. Diagnostic Imaging--methods--Atlases. 2. Nuclear Medicine--methods--Atlases.
3. Radiopharmaceuticals--Atlases. WN 39]
RC78.7.D53 D5282 2015
616.07/57--dc23

International Standard Book Number: 978-0-323-37753-9

Cover Designer: Tom M. Olson, BA
Cover Art: Richard Coombs, MS

Printed in Canada by Friesens, Altona, Manitoba, Canada

Last digit is the print number: 9 8 7 6 5 4 3 2 1

Dedications

This book is dedicated to my family.
To Diane and Ted Bennett, who love me the most.
To Betsy, Sidney, and Lee Andrew Clark, the loves of my life.
To my extended family of friends, Dr. Kathryn Morton, Cecilia Vargas Ortega.
Nothing matters without all of you.
Thank you to everyone who works with Amirsys: Your professionalism, leadership, and vision created the Diagnostic Imaging series, of which we are all proud to be a part.
Arthur Gelsinger and Dr. Umesh Oza: You made this endeavor fun. Double thanks.

PB

While we have laboriously poured heart, soul, and spirit into this textbook to impart the leading edge of nuclear medical knowledge to the next generation, there has been an equally and painstaking devotion paid to us by loved ones and mentors that have dedicated time, wisdom, guidance, and advice that cannot, and should not, go unrecognized. To my beautiful wife, Komel, thank you for your strength, guidance, and unwavering resolve. To my children, Quaid and Willa, you are my driving force. I want for you what you have given me — courage to strive for better, enjoy life to the absolute fullest, and run with wild abandon. To my loving parents, Dhruv and Surekha, thank you for your lifelong sacrifice, instilling discipline and confidence and single-minded focus raising three successful children. To Rishi and Veena, thank you for your unconditional love and steadfast support. A project of this magnitude reflects the hard efforts of many underrecognized people. I extend my deepest gratitude to all of you — thank you!

UDO

Contributing Authors

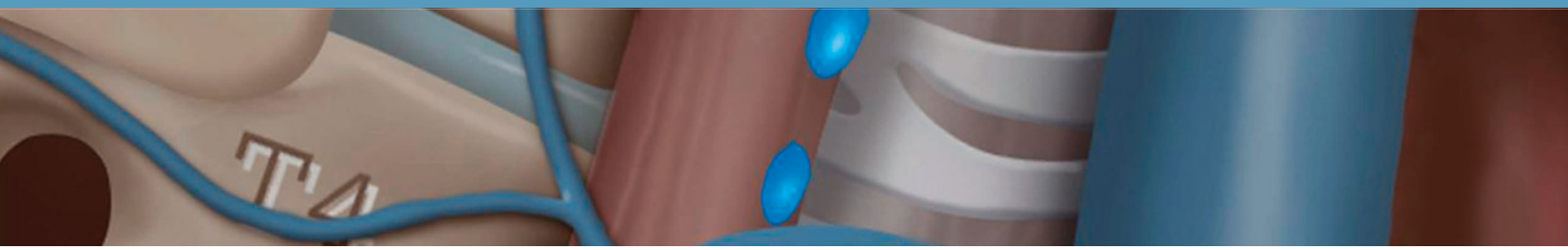

Angela P. Bruner, PhD, DABR
Director, Radiation Safety Officer, Medical Physicist
Radiation Safety & Medical Physics
Baylor Scott & White Health - North Texas
Dallas, Texas

Hollins Clark, MD
Associate Professor
Department of Radiology
Wake Forest School of Medicine
Winston-Salem, North Carolina

Pushpender Gupta, MBBS
Assistant Professor
Department of Radiology
Wake Forest School of Medicine
Winston-Salem, North Carolina

John M. Holbert, MD, FACR
Professor of Diagnostic Radiology
Department of Radiology
Wake Forest School of Medicine
Winston-Salem, North Carolina

Brian Kouri, MD
Associate Professor
Department of Radiology
Wake Forest School of Medicine
Winston-Salem, North Carolina

Shane C. Masters, MD, PhD
Assistant Professor
Department of Radiology
Wake Forest School of Medicine
Winston-Salem, North Carolina

Anita Thomas, MD
Associate Professor
Department of Radiology
Wake Forest School of Medicine
Winston-Salem, North Carolina

Christopher T. Whitlow, MD, PhD, MHA
Section Head, Neuroradiology
Associate Professor
Department of Radiology
Wake Forest School of Medicine
Winston-Salem, North Carolina

Matthew Bennett, MD
Department of Radiology
Wake Forest Baptist Medical Center
Winston-Salem, North Carolina

Todd Michael Danziger, MD
Department of Radiology
Wake Forest Baptist Medical Center
Winston-Salem, North Carolina

James Patrick Davidson, MD
Department of Radiology
Wake Forest Baptist Medical Center
Winston-Salem, North Carolina

Trevor Downing, MD
Department of Radiology
Wake Forest Baptist Medical Center
Winston-Salem, North Carolina

Christopher R. McAdams, MD
Department of Radiology
Wake Forest Baptist Medical Center
Winston-Salem, North Carolina

Amie M. McPherson, MD
Department of Radiology
Wake Forest Baptist Medical Center
Winston-Salem, North Carolina

Virginia Barnes Planz, MD
Department of Radiology
Wake Forest Baptist Medical Center
Winston-Salem, North Carolina

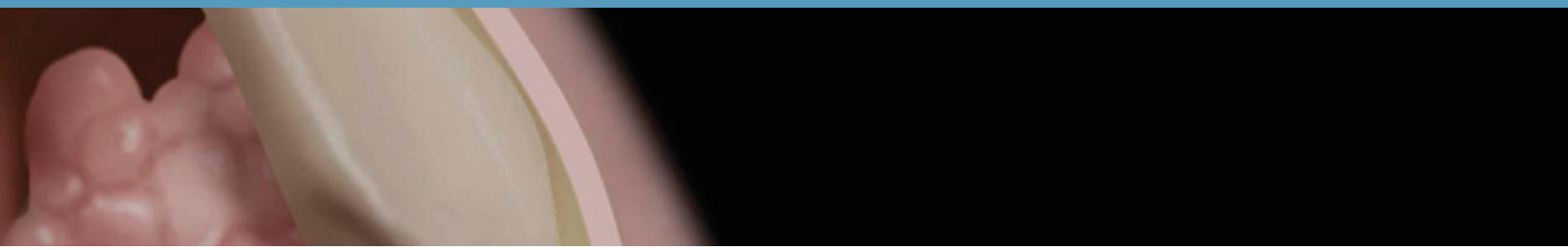

Colin Segovis, MD, PhD
Department of Radiology
Wake Forest Baptist Medical Center
Winston-Salem, North Carolina

Valerie E. Stine, MD
Department of Radiology
Wake Forest Baptist Medical Center
Winston-Salem, North Carolina

Pavani Thotakura, MD
Department of Radiology
Wake Forest Baptist Medical Center
Winston-Salem, North Carolina

Paula Vergara-Wentland, MD
Department of Radiology
Wake Forest Baptist Medical Center
Winston-Salem, North Carolina

Bimal Vyas, MD, MS
Department of Radiology
Wake Forest Baptist Medical Center
Winston-Salem, North Carolina

Amanda Jo Lott Marcellino, MD
Department of Otolaryngology
Wake Forest Baptist Medical Center
Winston-Salem, North Carolina

Ashley C. Mays, MD
Department of Otolaryngology
Wake Forest Baptist Medical Center
Winston-Salem, North Carolina

T. Alex McKnight, MD
Department of Otolaryngology
Wake Forest Baptist Medical Center
Winston-Salem, North Carolina

Kelli Y. Ha, MD
Department of Radiology, Breast Imaging
Baylor University Medical Center
Dallas, Texas

Tejaswini Vasamsetty, MD
Research Assistant
Department of Radiology
Wake Forest School of Medicine
Winston-Salem, North Carolina

John Bailey, MD
Wake Forest School of Medicine
Winston-Salem, North Carolina

Aidan Burke, MD
Wake Forest School of Medicine
Winston-Salem, North Carolina

Daniel G. Hampton, MD
Wake Forest School of Medicine
Winston-Salem, North Carolina

Katarina Kesty, MD, MBA
Wake Forest School of Medicine
Winston-Salem, North Carolina

Zachary Allen Lindsey, MD
Wake Forest School of Medicine
Winston-Salem, North Carolina

Charlotte Myers, MD
Wake Forest School of Medicine
Winston-Salem, North Carolina

Bryan J. Neth, BS
Wake Forest School of Medicine
Winston-Salem, North Carolina

Brad Perry, MD
Wake Forest School of Medicine
Winston-Salem, North Carolina

G. Lance White, MD
Wake Forest School of Medicine
Winston-Salem, North Carolina

Preface

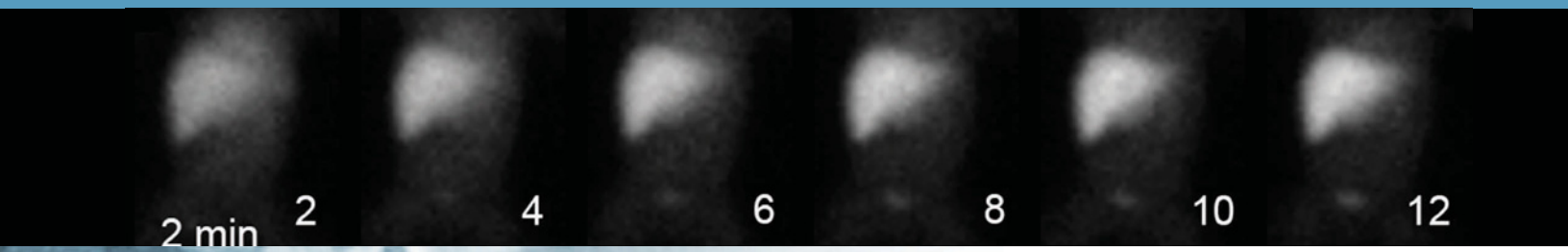

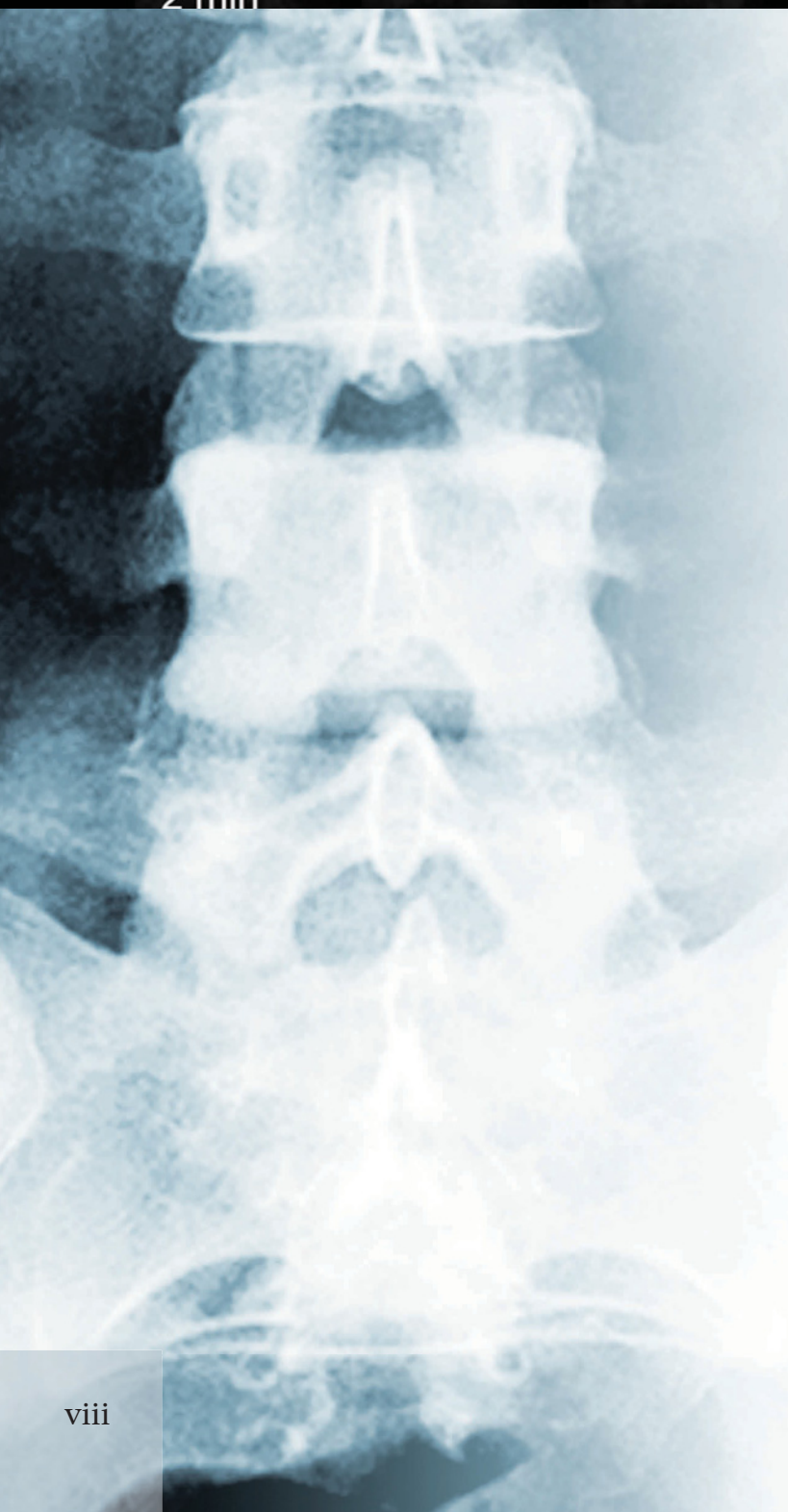

Since the publication of the first edition of *Diagnostic Imaging: Nuclear Medicine*, the world of nuclear medicine and molecular imaging has continued to rapidly evolve. PET/CT remains the most substantial advancement in the field in recent times, with PET/CT volumes continuing to climb. New PET/CT radiopharmaceuticals and time-of-flight technology have both become more mainstream. Astounding leaps have occurred in equipment such as with the incredible integrated PET/MR systems. Awareness of radiation dose to the patient has moved to the forefront of consciousness, and advances in software and detector equipment have helped dramatically lower radiation exposure. At the same time, many new therapies, radiotracers, and techniques push the boundaries of what is possible, showing the enduring importance of nuclear medicine in patient care.

The second edition reflects the changes seen in practice. Careful attention has been paid to the recent revisions in radioiodine therapy guidelines for cancer and hyperthyroidism. New chapters have been added, which cover the use of Ra-223 for the treatment of painful prostate cancer bone metastases and the use of I-123 ioflupane (DaTscan) for the diagnosis of parkinsonian syndromes. F-18 NaF PET/CT assessment for the bones is now thoroughly covered, including its indication for nonaccidental trauma in children. In addition, many of the popular quick reference tables have been added. These include easy-to-use tables in the completely updated pulmonary embolism chapter and differential diagnosis tables such as in the musculoskeletal chapters.

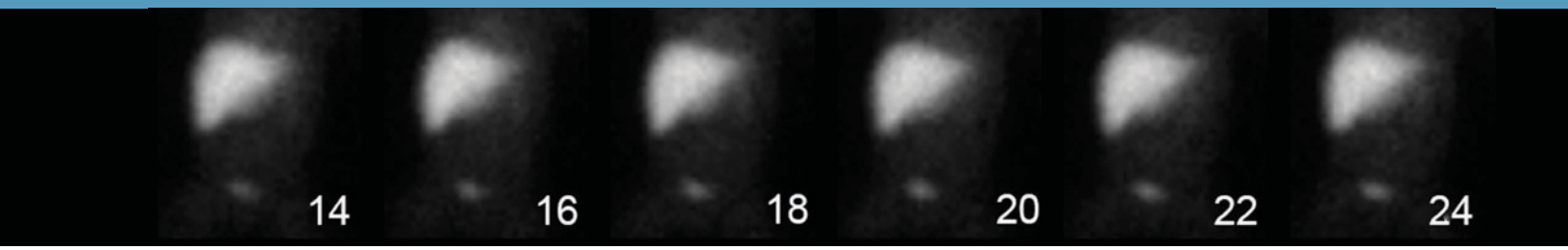

In order to make this text a more complete reference and study tool, new chapters have been dedicated to nuclear medicine physics and Nuclear Regulatory Commission (NRC) guidelines. In fact, all study guide topics listed for the American Board of Radiology board exam are fully covered. A radiopharmaceutical table now provides a critical overview, covering key parameters of the important agents currently in use. While these items are especially valuable for the physician preparing to undergo recertification or certification, they are also useful for the practitioner in the field.

Certainly, this edition continues to build on the successful philosophy of its predecessor. The topic-based format allows the reader to rapidly approach cases from the most practical standpoint. Incredible images illustrate the spectrum of disease, highlight potential pitfalls in the differential diagnosis, and outline critical anatomy. Each section contains multiple new images, maintaining the high standards expected from the *Diagnositc Imaging* series. Bulleted text describes all the details needed, from the level of the novice to that of the expert, but keeps the focus of each section sharp. Expanded sections have been added to better cover image interpretation and exam protocol advice, making this edition even more useful as a reference in the clinic.

We are especially proud of the team assembled to compile this text. They are a group of dedicated nuclear medicine physicians and nuclear radiologists who are also gifted teachers. Under the leadership of Dr. Paige Bennett (formerly Clark) of Wake Forest University Health Sciences and Dr. Umesh Oza of Baylor University, the text continues to be carefully edited and thoughtfully developed. In short, *Diagnostic Imaging: Nuclear Medicine, Second Edition*, continues to be a must-have for any practioner in the field.

Janis Petrik O'Malley, MD

Professor of Radiology
Director, Division of Molecular Imaging and Therapeutics
University of Alabama at Birmingham School of Medicine
Birmingham, Alabama

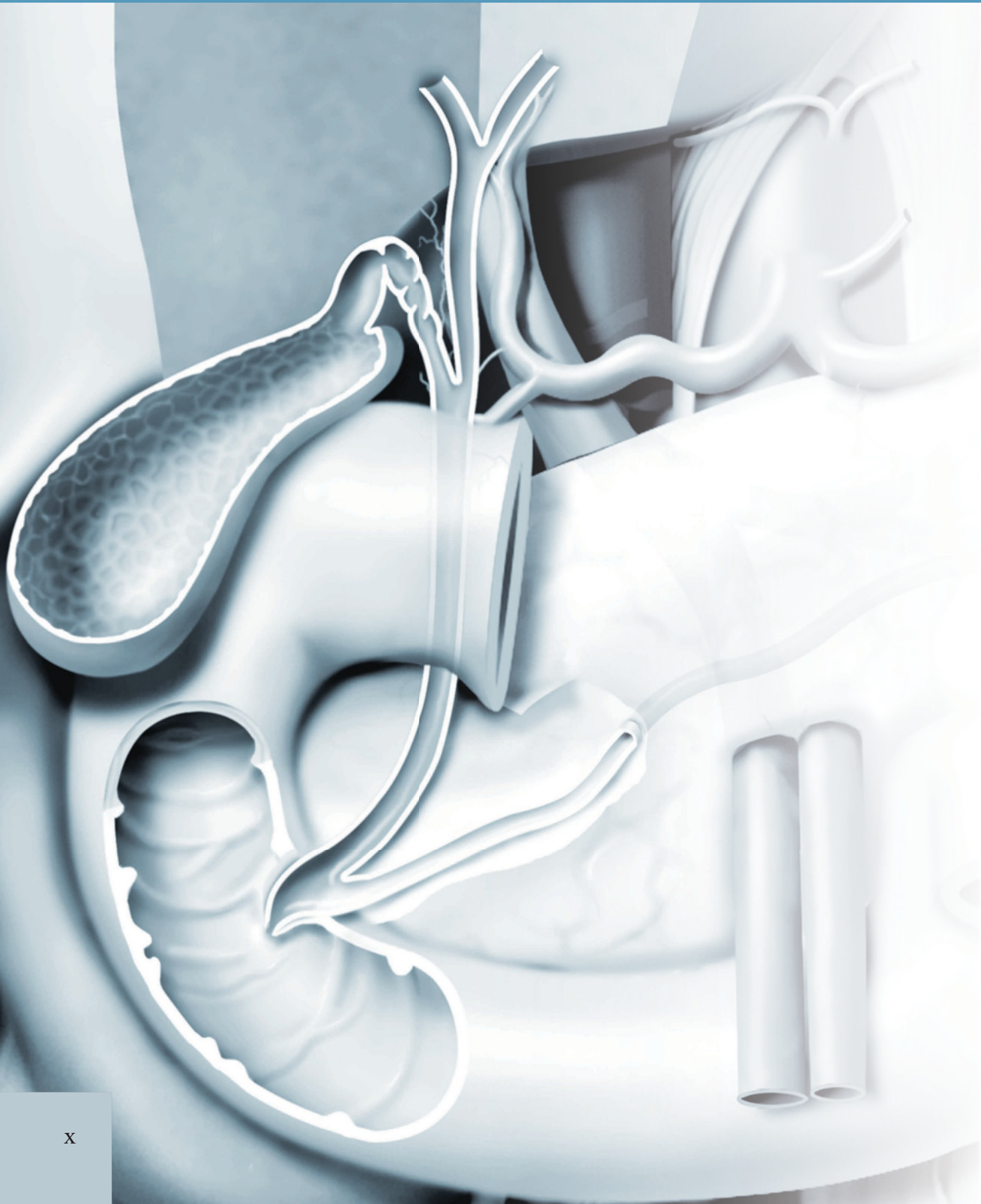

Acknowledgements

Text Editors

Nina I. Bennett, BA
Sarah J. Connor, BA
Tricia L. Cannon, BA
Terry W. Ferrell, MS
Lisa A. Gervais, BS
Karen E. Concannon, MA, PhD

Image Editors

Jeffrey J. Marmorstone, BS
Lisa A. M. Steadman, BS

Medical Editors

Philippe A. Tirman, MD
Whitney J. Morgan, MD

Illustrations

Richard Coombs, MS
Lane R. Bennion, MS
Laura C. Sesto, MA

Art Direction and Design

Tom M. Olson, BA
Laura C. Sesto, MA

Lead Editor

Arthur G. Gelsinger, MA

Production Coordinators

Angela M. G. Terry, BA
Rebecca L. Hutchinson, BA

ELSEVIER

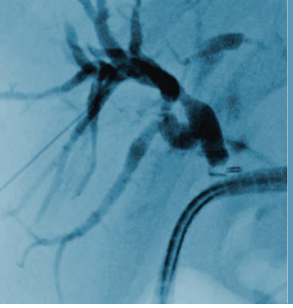

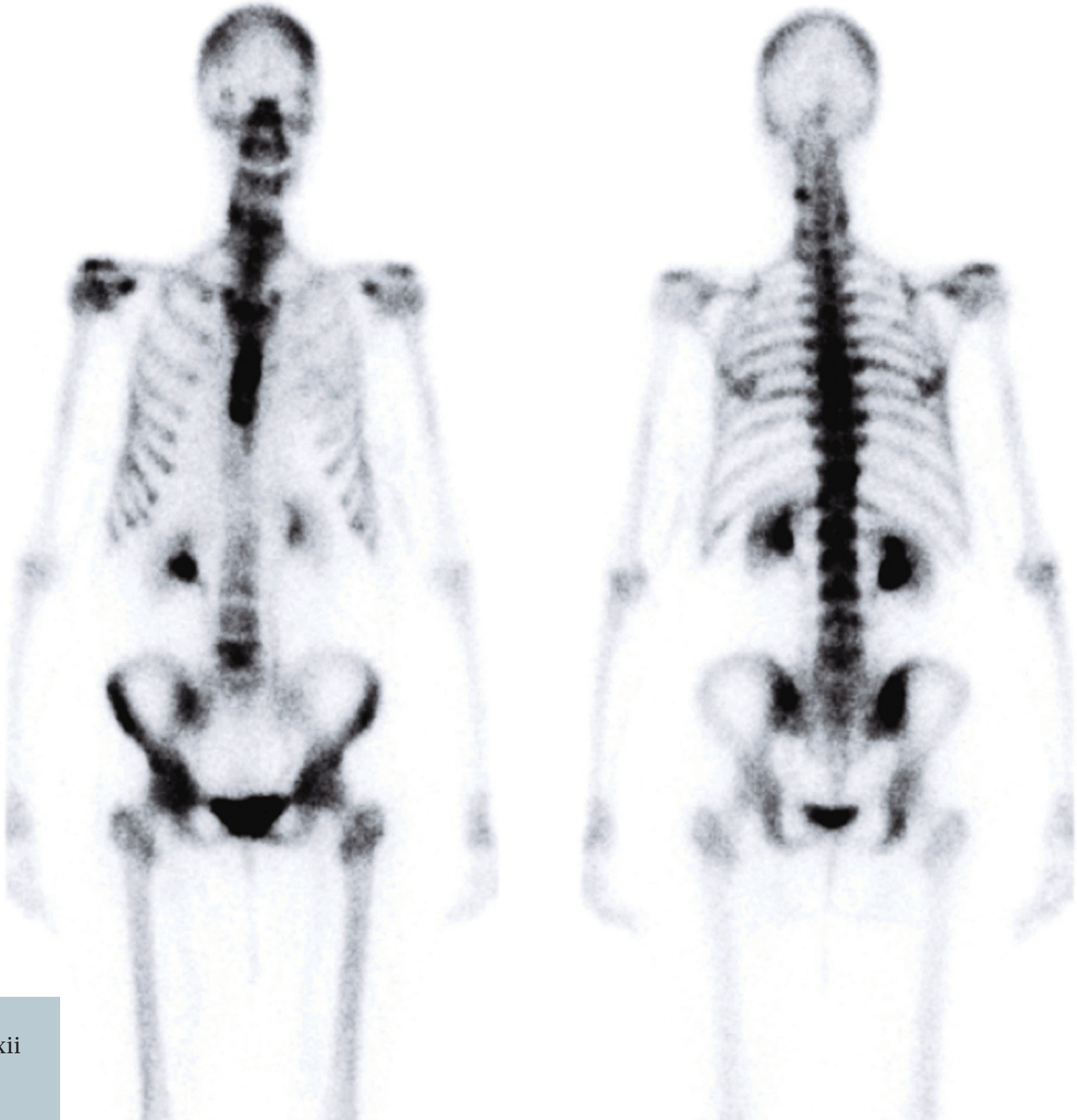

Sections

TABLE OF CONTENTS

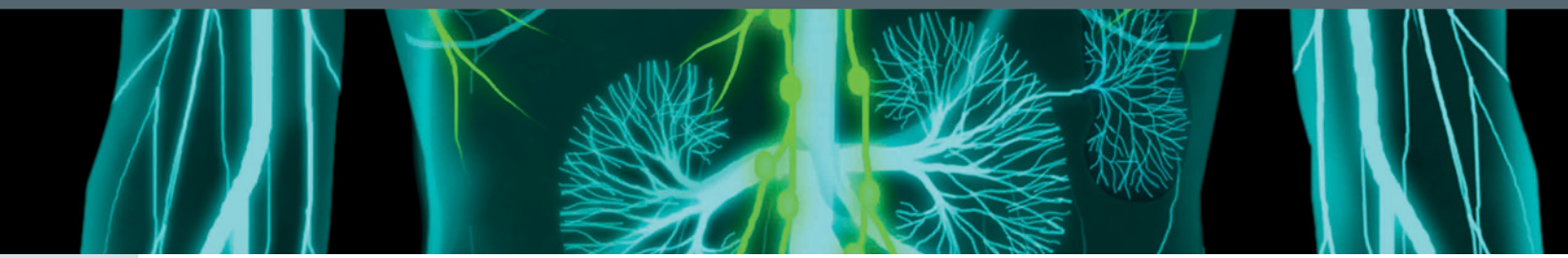

TABLE OF CONTENTS

TABLE OF CONTENTS

TABLE OF CONTENTS

TABLE OF CONTENTS

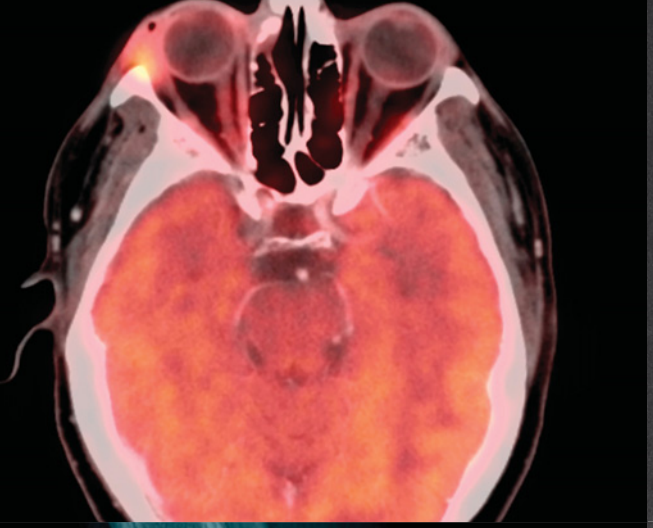

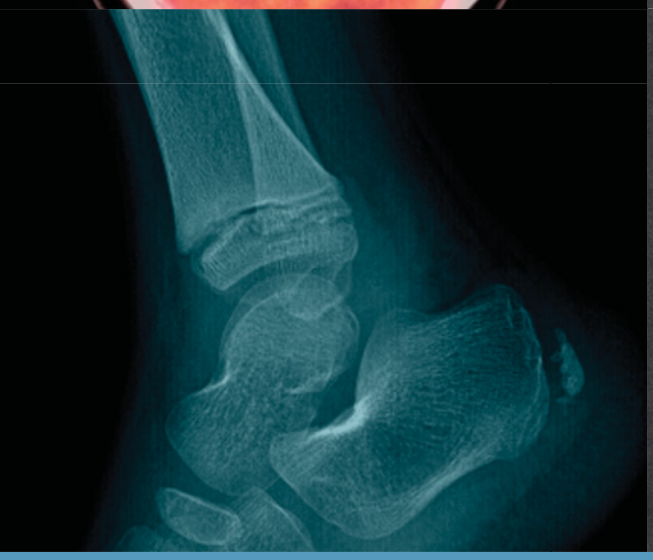

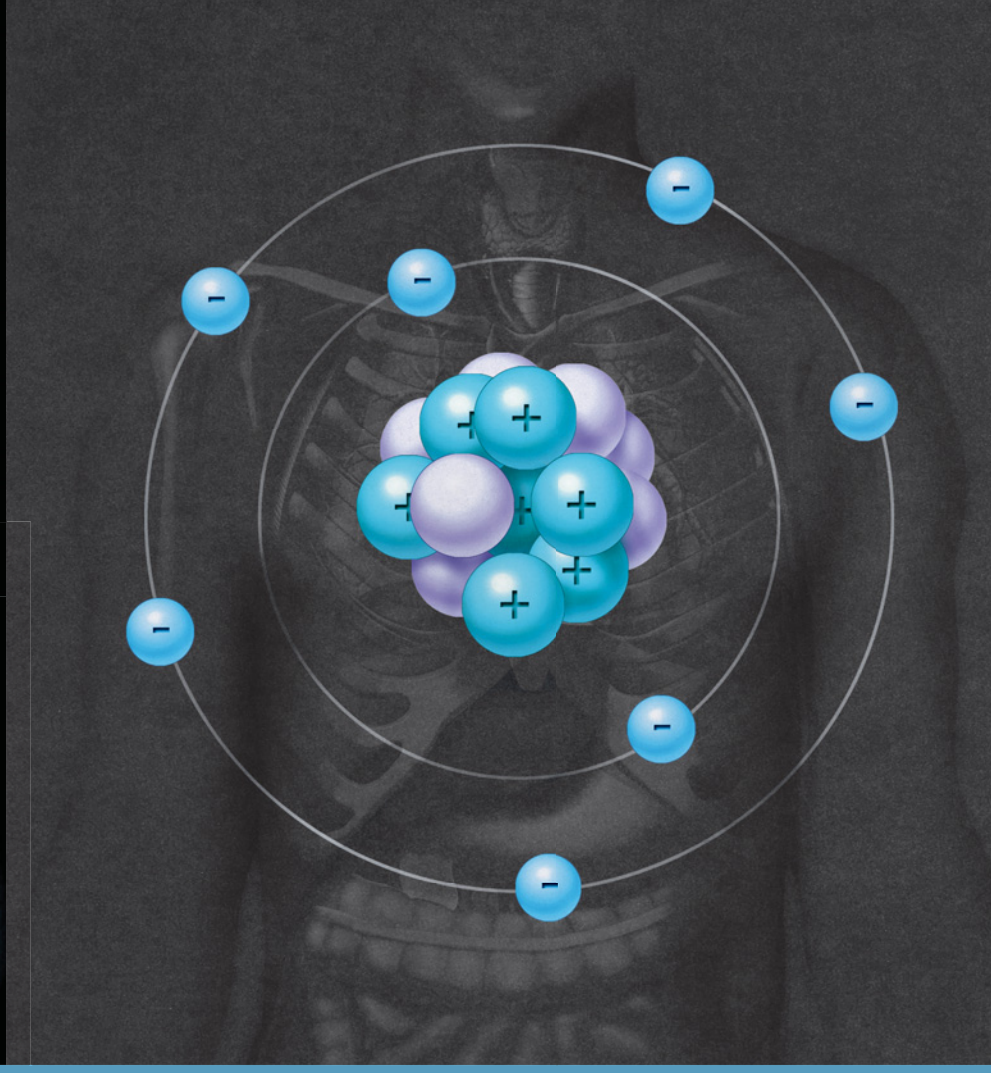

Diagnostic Imaging

Nuclear Medicine

SECOND EDITION

This page intentionally left blank

SECTION 1

Cardiac

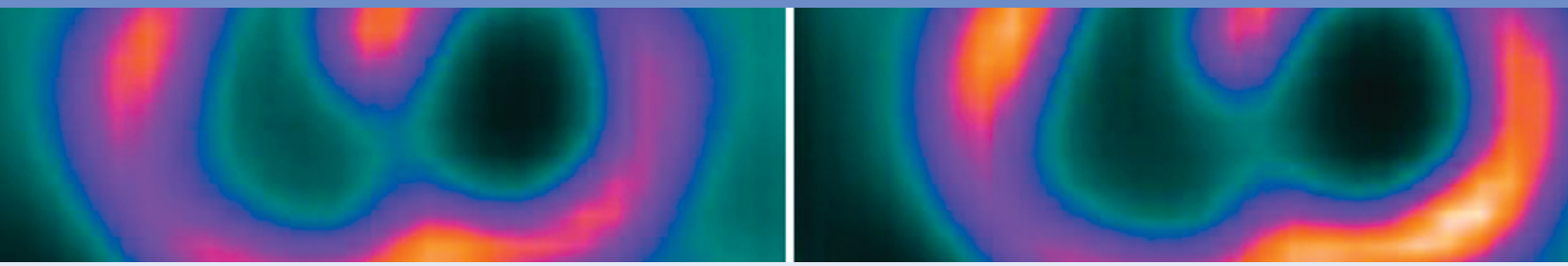

Introduction

Function and Coronary Artery Disease

Nuclear Cardiac Imaging

Nuclear cardiology encompasses studies that diagnose and risk stratify coronary artery disease, myocardial infarction and hibernation, left ventricular function, and detection of right-to-left shunt.

Myocardial perfusion imaging evaluates myocardial perfusion at rest and stress, diagnosing regional or global ischemia and myocardial infarction. In 1 meta-analysis of ~ 39,000 patients, patients with normal or low-risk patterns (e.g., mild reversible perfusion abnormalities in 1 vascular territory) on myocardial perfusion imaging had a 0.6% rate of cardiac death or myocardial infarction per year. In patients with moderate or severe reversible perfusion defects, the cardiac event rate was 6% per year, a much higher rate compared with low-risk or normal scans.

Myocardial perfusion imaging provides risk stratification in symptomatic and asymptomatic patients. Patients at high risk for coronary artery disease include those with diabetes mellitus, hyperlipidemia, hypertension, and a family history of coronary artery disease. If patients with risk factors are asymptomatic, myocardial perfusion imaging provides additional clinical information predicting cardiac events. For example, in asymptomatic diabetic patients with moderate or large perfusion defects, the event rate is 2.4% per year compared with a 0.4% per year event rate in patients with mildly abnormal or normal perfusion scans.

Evidence of severe disease on myocardial perfusion imaging correlates with an annual death rate of 2.9% to 4.2%. Evidence of high-risk disease includes 2-vessel reversible perfusion defects, transient ischemic dilatation (signifying global subendocardial ischemia), and lung uptake on Tl-201 studies.

Stress protocols with myocardial perfusion imaging are tailored to the clinical situation. Exercise stress protocol utilizing the modified Bruce protocol is used when possible. Note that with myocardial perfusion imaging, exercise stress tests are less valuable in patients with left bundle branch block, as this can cause a false-positive reversible perfusion defect in the septum. Pharmacologic stress protocols can be utilized in those patients unable to exercise. Vasodilator stress agents such as adenosine, regadenoson, and dipyridamole are most commonly used, followed by dobutamine if vasodilator stress is contraindicated.

Assessment of myocardial viability can be performed using Tl-201 and F-18 FDG PET/CT. In patients found to have underperfused yet viable or hibernating myocardium, regional wall motion is expected to improve after revascularization. One meta-analysis of ~ 3,000 patients with viable segments showed a 79% reduction in annual mortality after revascularization.

Nuclear cardiac imaging also has a role in risk stratification and management of patients with heart failure. Left ventricular function can be assessed using gated acquisitions of left ventricular function on myocardial perfusion imaging or with Tc-99m-labeled red blood cells (also called MUGA). Left ventricular ejection fractions using MUGA have been shown to have less inter- and intraobserver variability than other modalities, making it especially useful in serial determinations in patients undergoing chemotherapy.

Finally, when anatomic evaluation fails to diagnose a suspected right-to-left cardiac shunt, an indirect method of diagnosis can be obtained using nuclear medicine. If extrapulmonary localization of the pulmonary perfusion tracer Tc-99m MAA occurs, a right-to-left cardiac shunt is diagnosed.

Imaging Protocols

Myocardial Ischemia and Infarction

Cardiac radiotracers are taken up by the myocardium in proportion to cardiac blood flow. Images are obtained at rest and stress, then compared. Perfusion defects at stress that are not present at rest constitute inducible ischemia. Fixed perfusion defects at stress and rest signify myocardial infarction &/or myocardial hibernation.

Imaging protocols include single- and dual-isotope studies with Tc-99m-based perfusion agents &/or Tl-201 or PET/CT perfusion studies using Rb-82. Imaging with single-photon radiopharmaceuticals and gamma cameras is much more available clinically and less expensive than PET/CT myocardial perfusion imaging. In general, imaging with Tl-201 is used less commonly due to poorer imaging characteristics and dosimetry considerations as compared to Tc-99m-based radiopharmaceuticals.

Myocardial Viability

Myocardial viability can be assessed though Tl-201 rest-redistribution studies and F-18 FDG PET/CT. Tl-201 employs traditional gamma camera technology, 1 dose of radiopharmaceutical, and requires limited patient preparation. F-18 FDG PET/CT imaging of anaerobic glycolysis in hibernating, nonperfused myocardium is common, but requires recent meal and endogenous insulin response or exogenous insulin administration prior to F-18 FDG administration and PET/CT imaging. In addition, the F-18 FDG PET/CT data must be compared with a resting nuclear myocardial perfusion study, either a Tc-99m-based perfusion agent or Tl-201.

LV Function

Left ventricular function can be assessed with left ventriculography using Tc-99m-labeled red blood cells (traditionally called a MUGA scan) or gated myocardial perfusion scintigraphy, usually performed to diagnose cardiac ischemia. End-diastolic and end-systolic counts or volumes are utilized to calculate the left ventricular ejection fraction. Visual analysis of both types of studies allows for visual and quantitative analysis of regional and global left ventricular wall motion.

Right-to-Left Cardiac Shunt

To diagnose a suspected right-to-left cardiac shunt, a Tc-99m MAA pulmonary perfusion study is performed, with anterior and posterior images over the head, chest, and abdomen. In cases of right-to-left shunt, Tc-99m MAA will be present in the brain, lungs, and kidneys.

Practice Guidelines

The American Society of Nuclear Cardiology publishes clinical guidelines and quality standards for appropriate use, imaging, and reporting of nuclear cardiology studies. Content can be found online at www.asnc.org.

Selected References

1. Society of Nuclear Medicine and Molecular Imaging. ACR-SNMMI-SPR Practice Guideline for the Performance of Cardiac Scintigraphy. https://www.snmmi.org/ClinicalPractice/content.aspx?ItemNumber=6414#Cardio. Published October 1, 2009. Accessed July 31, 2015

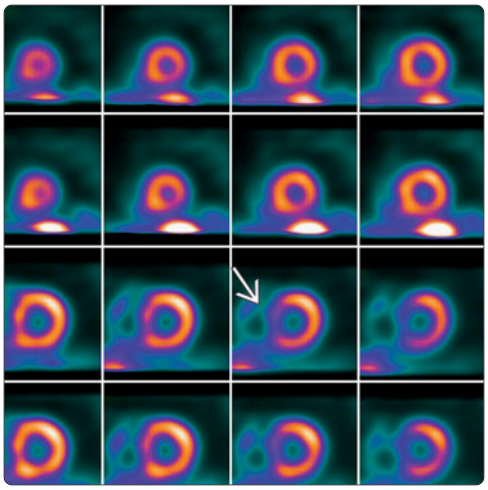

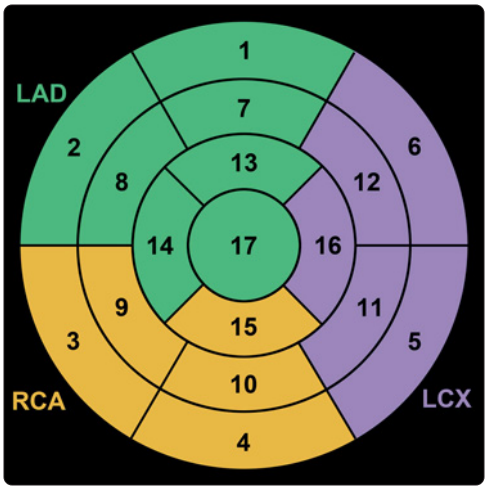

(Left) *This myocardial perfusion scan shows short-axis images of the left ventricle at stress (top) and rest (bottom). Note decreased activity in the membranous septum ➡, a normal finding.* **(Right)** *This graphic shows a short-axis bull's-eye of the left ventricle depicting the 17 segments and the associated vascular supply. These segments are used when reporting nuclear cardiology studies.*

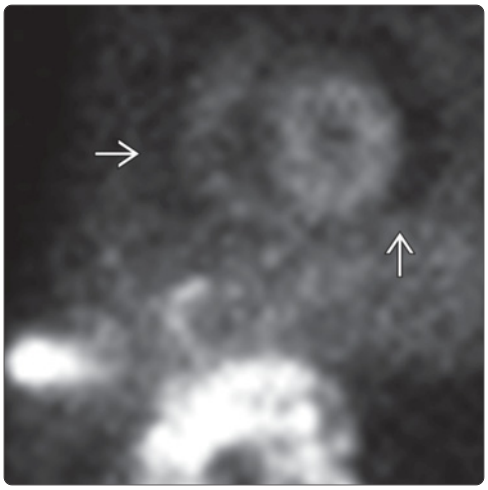

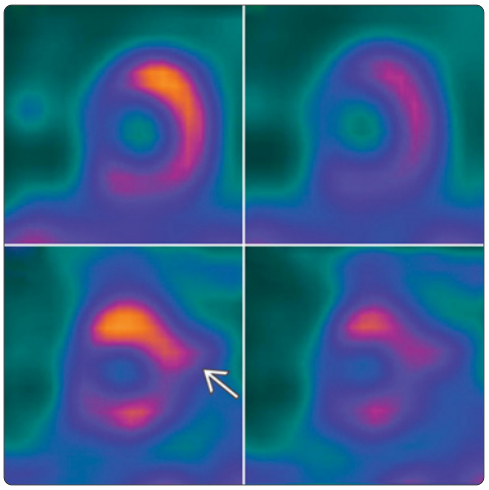

(Left) *Left anterior oblique raw image from a myocardial perfusion scan shows a photopenic defect around the heart ➡, corresponding to a pericardial effusion.* **(Right)** *Short-axis myocardial perfusion scan at stress (top) and rest (bottom) shows the "hurricane" sign ➡, an artifact caused by patient motion during the rest image acquisition.*

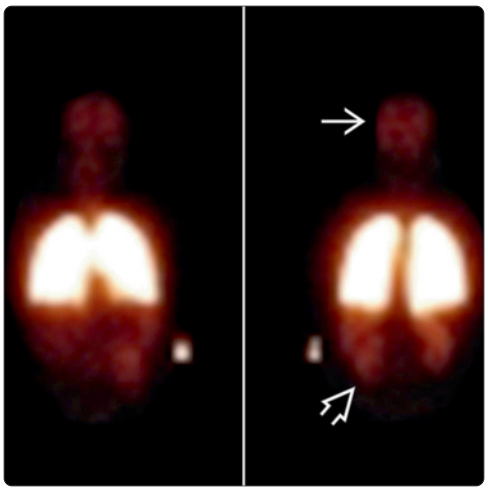

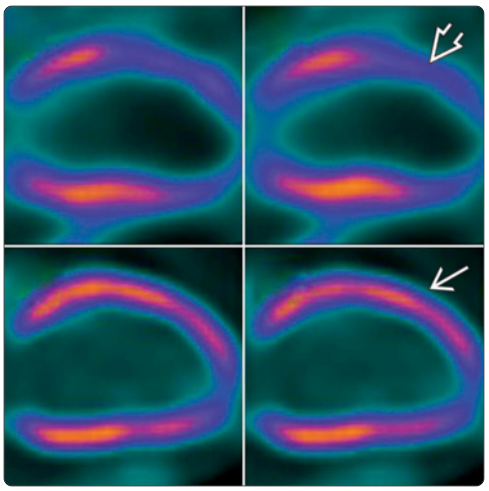

(Left) *Anterior and posterior Tc-99m MAA shunt study shows brain ➡ and kidney ➡ uptake, signifying a right-to-left cardiac shunt.* **(Right)** *Vertical long-axis F-18 FDG PET cardiac viability study shows uptake ➡ in a segment of hibernating myocardium ➡ on perfusion imaging. Revascularization of this region should improve myocardial contractility.*

KEY FACTS

IMAGING

- Multiple-gated cardiac blood pool acquisition (MUGA)
  - Low inter- and intraobserver variability (< 5%)
  - High reproducibility
- Radiopharmaceutical
  - 15-25 mCi (555-925 MBq) Tc-99m pertechnetate autologous labeled red blood cells (RBCs) IV
  - In vitro RBC labeling: Highest binding of radionuclide (~ 98%)
  - In vivo RBC labeling: > 80% binding
  - ROIs drawn around left ventricle
    - End systole, end diastole, and background
  - Heart must be in regular rhythm for optimal imaging
  - If background drawn over spleen or aorta, ejection fraction (EF) spuriously high
  - If background drawn over stomach or outside body, EF spuriously low
  - High unbound Tc-99m pertechnetate with recent transfusion, renal failure, heparin therapy, some chemotherapy, other medications

DIAGNOSTIC CHECKLIST

- Evaluate raw images (cine) for study quality
  - Counts, labeling, gating, views
- Compare qualitative estimation of left ventricular ejection fraction with quantitative calculation
- Comparison with previous studies important: Regions of interest should be similar
- Evaluate
  - Pericardial silhouette
  - Chamber sizes
  - Hypo/akinesis
  - Filling defects
  - Aneurysm
  - Ejection fraction

(Left) *Left anterior oblique multiple-gated cardiac blood pool acquisition (MUGA) shows the right ventricle ⇨, pulmonary artery ⇨, aorta ⇨, and left ventricle ⇨.* **(Right)** *Left anterior oblique MUGA shows region of interest (ROI) analysis: End diastole ⇨, end systole ⇨, and background ⇨ ROIs.*

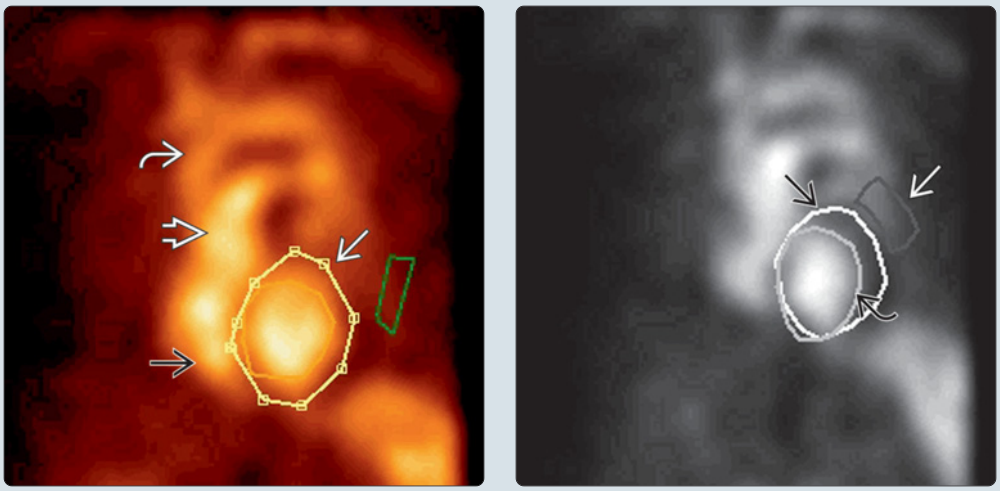

(Left) *Amplitude image demonstrates the degree or magnitude of contraction of the left ventricle. The red area ⇨ contracts the most.* **(Right)** *Phase image demonstrates the sequence of contraction of the heart, with the right ⇨ and left ventricles ⇨ showing similar colors since they contract simultaneously.*

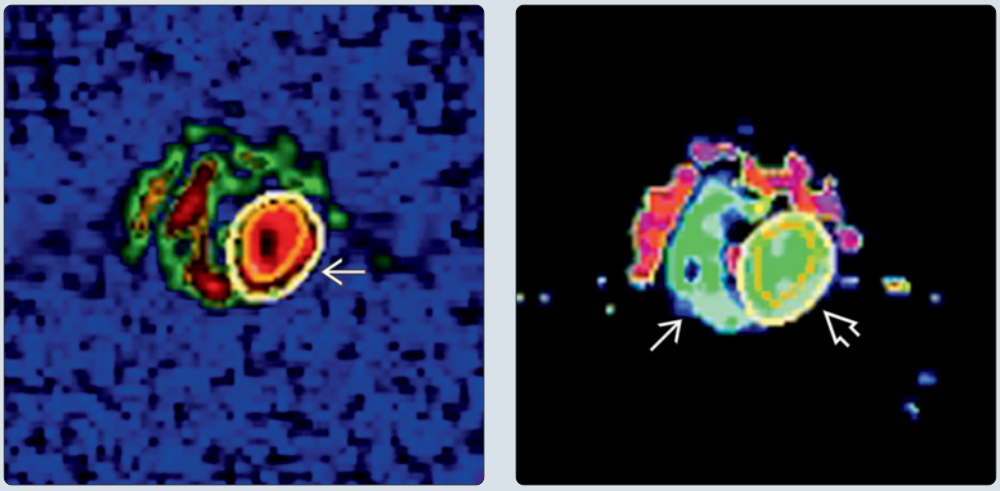

IMAGING

Imaging Recommendations

- Best imaging tool
  - Multiple-gated cardiac blood pool acquisition (MUGA)
  - Tc-99m labeled autologous red blood cells (RBCs)
    - Images obtained over heart
    - Analysis of counts at end diastole and end systole → left ventricular (LV) ejection fraction (EF)
  - Low inter- and intraobserver variability (< 5%)
  - High reproducibility
  - Excellent correlation with cardiac catheterization ventriculography (r = 0.94)
- Protocol advice
  - Patient prep: None
  - Radiopharmaceutical: 15-25 mCi (555-925 MBq) Tc-99m pertechnetate autologous labeled RBCs IV
    - In vitro RBC labeling
      - Highest binding of radionuclide (~ 98%)
      - Safety issues with reinjection of blood products
      - Contraindicated if heparin allergy
    - In vivo RBC labeling: > 80% binding
    - High unbound Tc-99m pertechnetate levels with recent transfusion, renal failure, heparin therapy, some chemotherapy, other medications
  - Dosimetry
    - Organ receiving largest radiation dose: Heart
  - Image acquisition
    - Patient supine
    - ECG gating
      - 16-32 frames per R-R interval
    - Planar images: LEAP/high-resolution collimator
    - Matrix: 64 x 64
    - Each image acquired for 300K counts or 5 min
    - Anterior view: 45° shallower than best septal LAO
      - Shows anterolateral and apical LV; right atrium and right ventricle
    - Best septal view LAO: Angle chosen that best shows septum between right and left ventricles
      - Shows septal, anterolateral, posterolateral LV
    - Left lateral/LPO: 45° greater than best septal LAO
      - Shows inferior, apical, anterolateral LV
    - Caudal angulation ± slanted collimator: May help separate ventricular from atrial blood pool
    - Image processing
      - Evaluate raw images (cine) for study quality: Counts, labeling, gating, views
  - Region of interest (ROI) analysis
    - ROIs drawn around LV: End systole, end diastole, and background
      - Manual, automatic, or semiautomatic ROI placement available
      - Avoid drawing background over spleen or aorta; EF will be spuriously high
      - Avoid drawing background over empty stomach or outside body; EF will be spuriously low
      - Background ~ 1/3 size of end diastole

Artifacts and Quality Control

- Heart must be in regular rhythm for optimal imaging
  - Irregular heartbeats rejected
    - Optimal: ≤ 10% irregular beats
    - Ejection fraction results less reliable if ≥ 30% irregular beats

DIFFERENTIAL DIAGNOSIS

Ischemic Dilated Cardiomyopathy

- Cardiovascular
  - Regional wall motion abnormalities in coronary artery distribution most common

Nonischemic Dilated Cardiomyopathy

- Toxic cardiomyopathy induced by chemotherapy
  - Serial LVEFs most common MUGA indication
- Also: Stress-induced, infectious, genetic, peripartum, sarcoid, autoimmune, cirrhosis, end-stage renal disease

DIAGNOSTIC CHECKLIST

Image Interpretation Pearls

- Compare qualitative estimation of LVEF with quantitative calculation
  - Reprocessing may be necessary if discrepancy
- Comparison with previous studies important: ROIs should be similar
  - Reprocessing may be necessary if discrepancy

Reporting Tips

- Cardiac morphology
  - Chamber sizes
  - Ventricular wall thickness
  - Pericardial silhouette
  - Filling defects
- Systolic function
  - Qualitative
    - Global LV function
    - Regional LV function
      - Hypo/akinesis, aneurysm
- Ejection fraction
  - Qualitative: Estimate from cine loop
  - Quantitative: ROI analysis of counts and calculation
    - LVEF (%): [End diastolic counts - background counts] - [end systolic counts - background counts] / [end diastolic counts - background counts] x 100
- Phase image: Shows sequence of contraction of atria and ventricles
- Amplitude image: Shows magnitude of contraction of atria and ventricles
- Right ventricular EF
  - Qualitative and quantitative analysis as with LVEF

SELECTED REFERENCES

1. American College of Radiology. ACR–SNM–SPR Practice Guideline for the Performance of Cardiac Scintigraphy, Resolution 14. http://snmmi.files.cms-plus.com/docs/Cardiac_Scintigraphy_1382731812393_3.pdf. Revised 2009. Accessed July 9, 2014

(Left) *Anterior MUGA shows right atrium, right ventricle, anterolateral left ventricle, and left ventricular apex.* **(Right)** *Anterior graphic of the heart shows right atrium, right ventricle, anterolateral left ventricle, and left ventricular apex.*

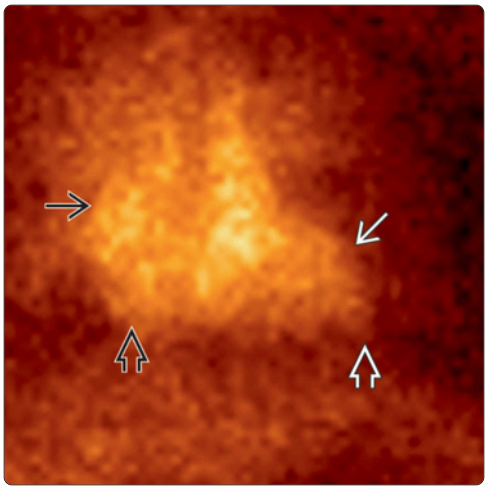

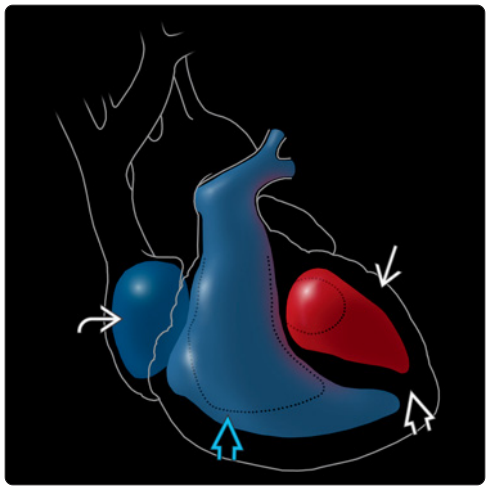

(Left) *Left anterior oblique MUGA shows septum, anterolateral left ventricle, and posterolateral left ventricle. Also called the best septal view, this image is commonly obtained at 45°. Caudal tilt can also assist in obtaining best view of septum.* **(Right)** *Left anterior oblique graphic of the heart shows right ventricle, septum, and left ventricle.*

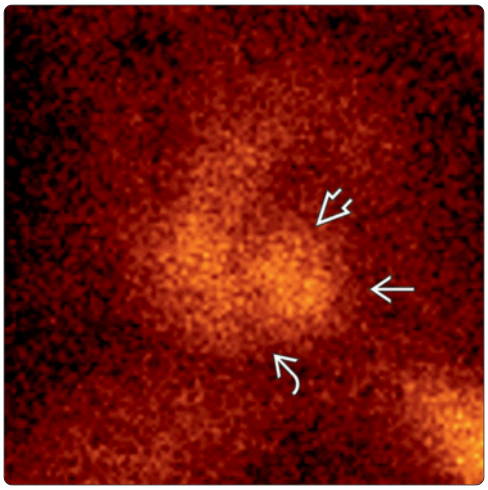

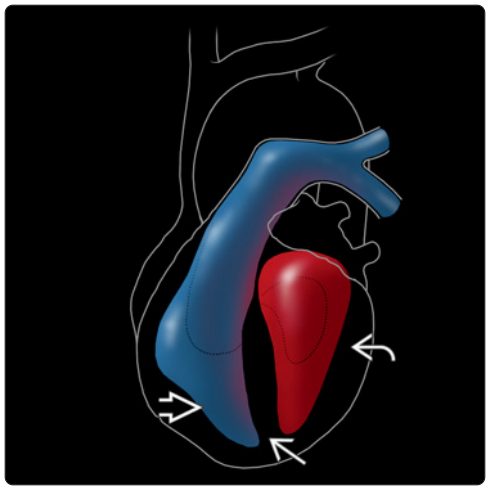

(Left) *Left posterior oblique MUGA shows inferior, apical, and anterolateral left ventricle. Note splenic activity, normal physiologic uptake on Tc-99m pertechnetate RBC studies.* **(Right)** *Left posterior oblique graphic of the heart shows inferior, apical, and anterolateral left ventricle.*

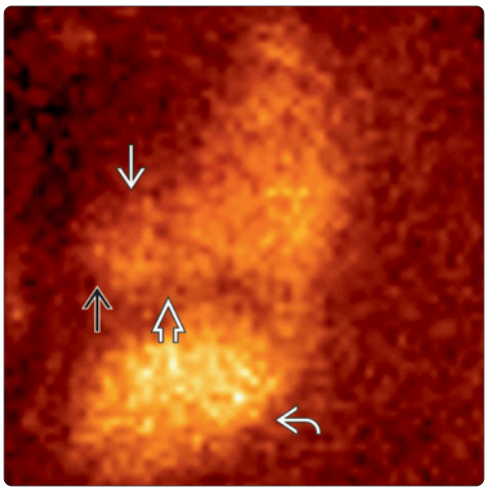

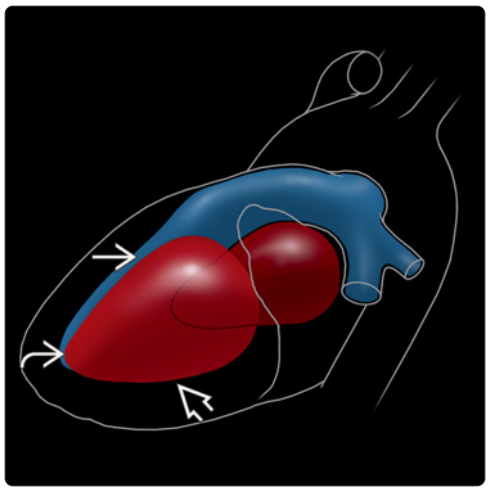

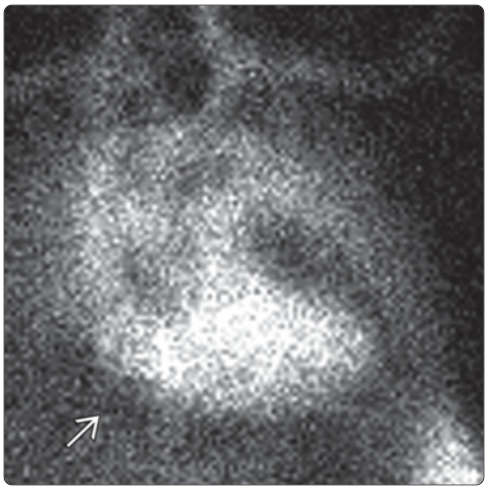

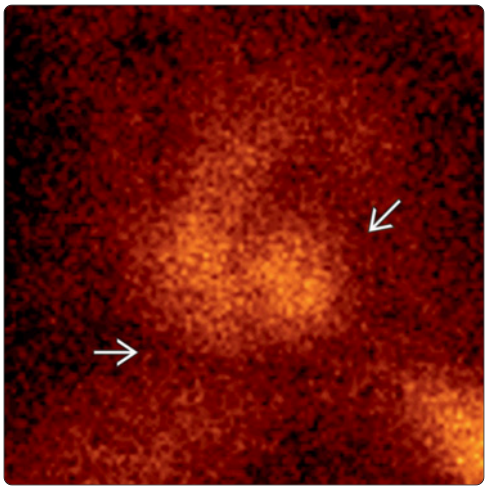

(Left) *Anterior MUGA shows a large photopenic defect* ➡ *surrounding the heart.* **(Right)** *Left anterior oblique MUGA in the same patient shows the photopenic defect* ➡ *around the heart, a large pericardial effusion.*

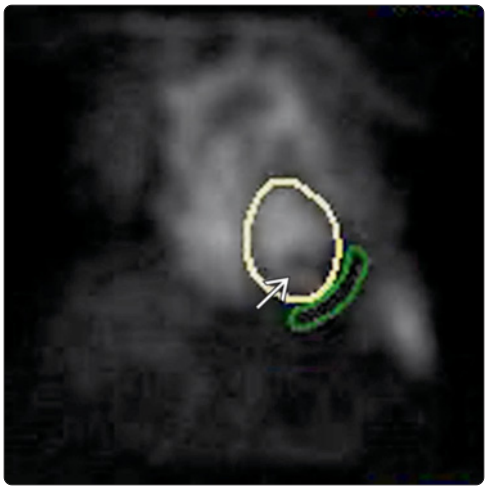

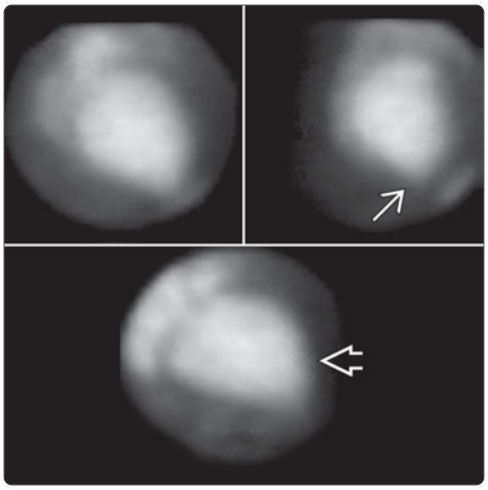

(Left) *Left anterior oblique MUGA shows a filling defect* ➡ *in the left ventricular apex. The differential diagnosis includes mass lesions and thrombus. Note that medical devices such as pacemakers and postmastectomy tissue expanders can cause artifactual filling defects on MUGA; however, these tend to be in different locations depending on the angle of imaging.* **(Right)** *This MUGA shows dilated left ventricle* ➡ *and LV dyskinesis* ➡ *apparent on end-systolic images, a small LV aneurysm.*

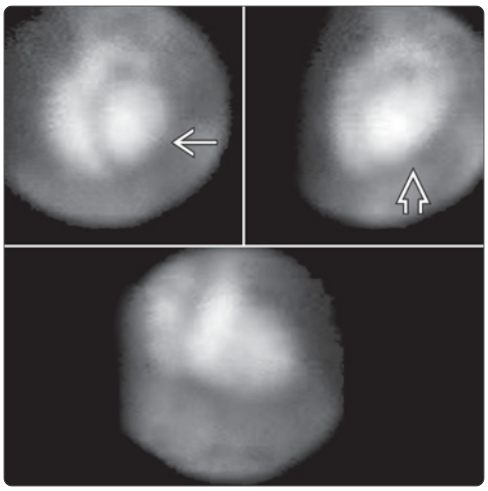

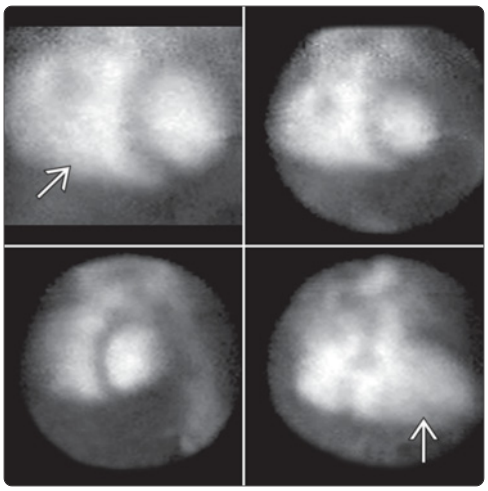

(Left) *This MUGA demonstrates dilated left ventricle and global hypokinesis, evidenced by minimal excursion between end diastole* ➡ *and end systole* ➡ *in a patient with chemotherapy-induced cardiomyopathy.* **(Right)** *This MUGA shows severe biventricular enlargement* ➡ *in a patient with viral-induced cardiomyopathy.*

KEY FACTS

DIAGNOSTIC CHECKLIST

- Raw images
  - May identify artifacts, extracardiac tracer uptake (cancer, infection, bowel), infiltration
- Study quality
  - Comment if excessive motion, poor radiotracer uptake/infiltration, technical error
- Artifacts
  - Motion, scatter, reconstruction, attenuation
- Adequacy of stress modality
  - Exercise or pharmacologic
- Perfusion images: Qualitative analysis
  - LV chamber size: Normal vs. dilated
  - 17 segment model: Describe stress/rest perfusion
  - Transient ischemic dilatation (TID): Dropout of endocardial border on stress
- Perfusion images: Quantitative analysis
  - 17 segment model: Each segment scored on 5-pt scale
  - Summed difference score: < 4 = normal; 4-8 = mildly abnormal; 9-13 = moderately abnormal; > 13 = severely abnormal
  - TID ratio: 1.12-1.36 positive for TID
- Gated images: Ejection fraction and wall motion
  - Brightening and endocardial excursion = normal
  - Hypokinesis/akinesis if photopenia, lack of endocardial excursion
  - Lower limits of normal EF for MPI: 45%
  - EF overestimated if small heart size
- Conclusion
  - Positive or negative for inducible ischemia
  - Positive or negative for myocardial infarction (± peri-infarct ischemia)
    - Consider possibility of hibernating myocardium, need for viability study
  - LV function: EF and wall motion

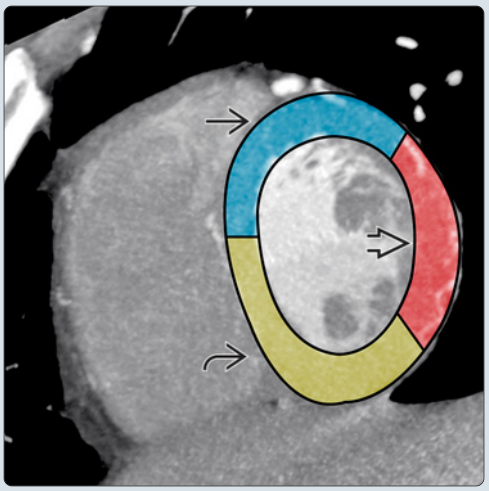

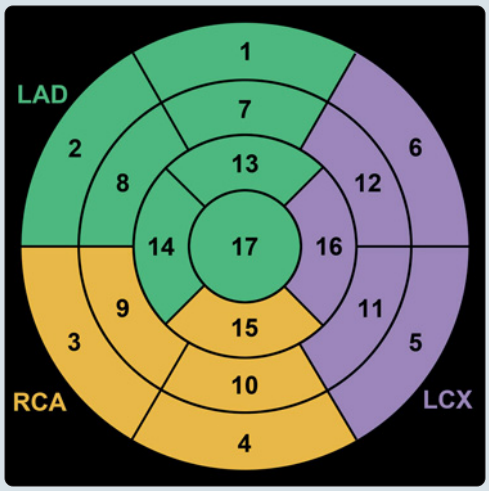

(Left) *Short axis view of the left ventricle on CT shows vascular territories supplying the myocardium. The left anterior descending artery supplies the anterior and septal walls. The left circumflex artery supplies the lateral wall. The right coronary artery supplies the inferior and inferoseptal walls.* **(Right)** *Drawing of short axis 17-segment model shows bull's-eye view of the heart for quantitative analysis.*

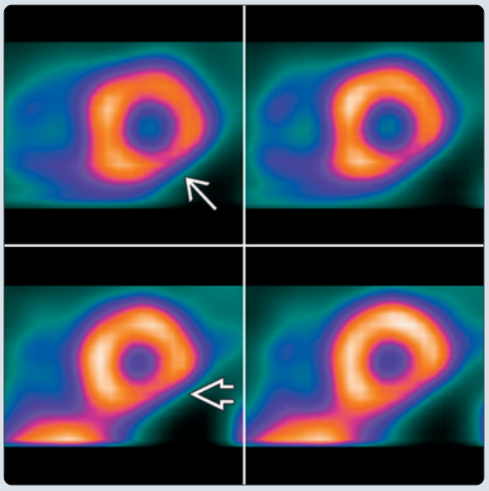

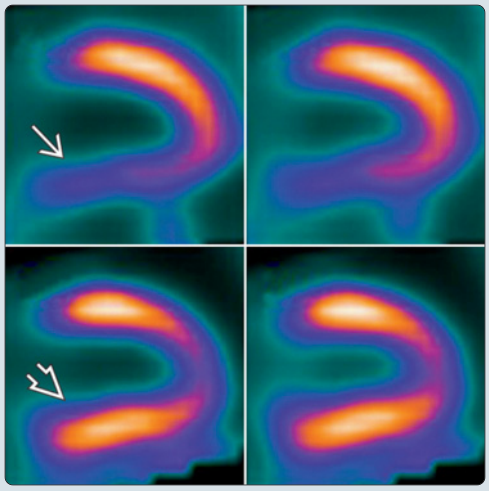

(Left) *Short axis MPI shows decreased activity in the inferolateral wall on rest, which is more pronounced on stress images, signifying inferolateral infarction with peri-infarct ischemia. Note the perfusion defect appears flat.* **(Right)** *Vertical long axis MPI shows inferior wall before attenuation correction on SPECT/CT. After attenuation correction, counts in the inferior wall are no longer artifactually decreased by diaphragmatic/soft tissue attenuation in this obese patient.*

IMAGING

General Features

- Best diagnostic clue
  - Myocardial perfusion imaging (MPI)
    - Usually Tc-99m-based perfusion agent that localizes to myocardium
      - Radiotracer injected at rest, then image
      - Radiotracer injected at stress, then image
      - Rest and stress images compared
    - Myocardial ischemia: Perfusion defect evident on stress images, normal perfusion on rest images
    - Acute myocardial infarction (AMI): Perfusion defect on MPI with injection within 2 hrs of pain episode
    - Chronic myocardial infarction: Fixed perfusion defect on rest and stress images
    - Hibernating myocardium: Fixed perfusion defect on rest/stress images, normal on viability images
- Location
  - Anterior/septal wall: Left anterior descending (LAD) artery
  - Lateral wall: Circumflex artery
  - Inferior wall: Posterior descending artery (PDA)
    - Right coronary artery (RCA) in 85% (right dominant)
    - Continuation of circumflex in 15% (left dominant)
  - Apex: Usually from LAD, but variable

Imaging Recommendations

- Protocol advice
  - Patient preparation
    - Review for contraindications to stress test, pregnancy
    - Mostly required for stress portion of test
      - NPO for 4 hrs prior to stress test
      - No caffeine 12 hrs prior to pharmacologic stress
  - Radiopharmaceutical
    - Tc-99m sestamibi or Tc-99m tetrofosmin
      - Dose: 10-40 mCi (370 MBq to 1.4 GBq)
      - 1-day protocol: Up to 40 mCi (1.4 GBq) (10 mCi [370 MBq] for rest, 30 mCi [1.1 GBq] for stress)
      - 2-day protocol (patients > 250-275 lbs): 25-30 mCi (925 MBq to 1.1 GBq) for both rest and stress, 1 day apart
      - Dosimetry: Colon (sestamibi) and gallbladder wall (tetrofosmin) receive largest radiation dose
      - 6 hrs t1/2
    - Thallium-201 chloride
      - Dose: 2-4 mCi (74-148 MBq)
      - Rest images on dual-tracer MPI
      - Stress-rest images on Tl-201 only MPI
      - Redistribution imaging for viability
      - Long t1/2 (73 hrs) leads to higher dose than Tc-99m-based agents
      - Dosimetry: Kidneys receive largest radiation dose
    - Rb-82
      - Dose: 2D PET: 40-60 mCi (1.4-2.2 GBq); 3D PET: 10-20 mCi (370-740 MBq) BGO system; 30-40 mCi (1.1-1.4 GBq) LSO system
      - Generator produced
      - 75 sec t1/2
      - Cost-effective PET tracer for high-volume centers
      - Pharmacologic stress utilized due to short t1/2
      - Dosimetry: Kidneys receive largest radiation dose
    - N-13 ammonia
      - Dose: 15-25 mCi (555-925 MBq)
      - PET perfusion agent
      - Cyclotron produced (on-site due to 9.8 min t1/2)
      - Dosimetry: Urinary bladder receives largest radiation dose
  - Image acquisition: Tc-99m sestamibi and Tc-99m tetrofosmin
    - Patient position: Supine, upright/semiupright
    - Injection to imaging time: 15-60 min
    - Time between rest/stress injections: 30 min to 4 hrs
    - Collimator: Low energy, high resolution
    - 180° planar acquisition: Preferred if no attenuation correction (better spatial resolution, higher contrast, less attenuation)
    - SPECT and SPECT/CT: Preferred in obese patients, allows attenuation correction
    - Matrix: 64 x 64
    - Step and shoot or continuous acquisition
    - 60-64 projections; 20-25 sec per projection
    - ECG gate stress only or rest and stress
    - 8 frames/cycle standard
    - 140 keV with 15-20% window
  - Image acquisition: Tl-201
    - Similar to Tc-99m-based tracers, except
      - 70-80 keV with 15-20% window
      - 64 projections
      - Stress-rest MPI: Image 10 min after injection for stress images; rest (redistribution) images at 3-4 hrs
      - Rest only for dual-tracer MPI: Image 10 min after injection for rest images; utilize Tc-99m-based radiotracer for stress
      - Viability: Image 10 min after injection for rest images; redistribution (viability) images at 3-4 hrs
  - Image acquisition: Rb-82 and N-13 ammonia PET/CT
    - Rb-82: Image acquisition starts 1-1.5 min after injection, 5-10 min acquisition
    - N-13 ammonia: Image acquisition starts 4-5 min after injection, 10-15 min acquisition
    - Attenuation correction from CT for large patients
  - Image processing
    - Reconstruction using filtered backprojection or iterative reconstruction
    - Stress images usually displayed on top row, rest images on bottom row

Artifacts and Quality Control

- Motion artifact
  - Hurricane sign: Counts outside epicardial border on short axis
  - Blurred endocardial border
  - Lateral wall blurring
- Scatter artifact
  - Counts scatter into inferior wall due to high bowel activity
- Reconstruction artifact
  - Photopenia in inferior wall from high bowel activity
  - Photopenia at 11 o'clock position on short-axis views on rest and stress

- Attenuation
  - Soft tissue attenuation causing fixed defects
  - Misregistration of attenuation correction map and perfusion data

DIFFERENTIAL DIAGNOSIS

Myocardial Infarction

- Normal apical thinning
- Left ventricular hypertrophy: Fixed lateral wall defect
- Soft tissue attenuation of photons: Breast (anterior wall), diaphragm (inferior wall)
- Septal hypokinesis common in absence of MI, especially after coronary artery bypass graft surgery
- Decreased activity in lateral wall on N-13 ammonia PET can be seen in healthy controls
- Myocardial hibernation: Myocardium with little/no perfusion, but viable due to anaerobic glycolysis
  - 25% of fixed defects are viable on viability studies

Myocardial Ischemia

- Artifactual perfusion defects on stress only (e.g., bowel activity on stress images, shift of overlying soft tissue)
- Left bundle branch block: Functional septal reversibility with exercise stress (false-positive)

Other Vascular Disease

- Vasospastic disease (Prinzmetal angina)
- Microvascular disease (e.g., diabetes mellitus, syndrome X)

PATHOLOGY

General Features

- Etiology
  - Ruptured coronary artery plaque disrupts myocardial blood supply
    - Myocardial necrosis begins in 20-30 min, spreading from subendo- to epicardium
  - Risk factors
    - Hyperlipidemia, diabetes mellitus, hypertension, obesity, cigarette smoking, family history

CLINICAL ISSUES

Demographics

- Age
  - Men: Usually > 45 yrs
  - Women: > 55 yrs

DIAGNOSTIC CHECKLIST

Consider

- Myocardial infarction
  - Fixed perfusion defect, regional wall motion abnormality
  - Peri-infarct ischemia can cause chest pain
- Myocardial ischemia
  - Reversible perfusion defect on rest and stress images, no regional wall motion abnormality

Reporting Tips

- Raw images
  - Review to identify artifacts, extracardiac radiotracer uptake (breast/lung cancer, lymphoma, infection)
- Study quality
  - Comment if excessive motion, poor radiotracer uptake/infiltration, technical error
- Artifacts
  - Describe if present: Motion, scatter, reconstruction, attenuation
- Adequacy of stress modality
  - Exercise: Discuss percent age-predicted max heart rate achieved
  - Vasodilators: If infused and radiotracer injected per protocol, assume adequate stress
- Perfusion images
  - Qualitative analysis
    - LV chamber size: Normal vs. dilated
    - 17 segment model: Describe perfusion defects on stress and rest using these segments
    - Transient ischemic dilatation (TID): Dropout of endocardial border on stress
  - Quantitative analysis
    - Quantitative perfusion analysis
      - Computer generation of segmental perfusion scores in each of 17 segments on a 5-point scale at stress and rest (0 = normal, 4 = absent)
      - Summed stress score (SSS): Analysis of resting and stress-induced perfusion defects
      - Summed rest score (SRS): Analysis of resting perfusion defects
      - Summed difference score (SDS): SSS minus SRS; a measure of stress-induced ischemia
      - SDS: < 4 = normal; 4-8 = mildly abnormal; 9-13 = moderately abnormal; > 13 = severely abnormal
    - TID ratio: 1.12-1.36 correlates with multivessel disease
      - TID = endocardial volume at stress / endocardial volume at rest
- Gated images
  - Wall motion
    - Normal if brightening and endocardial excursion on gated slice images
    - Hypokinesis/akinesis if photopenia, lack of endocardial excursion
  - Ejection fraction
    - Lower limits of normal for MPI: 45%
    - Overestimated if small heart size
- Conclusion
  - Positive or negative for inducible ischemia
  - Positive or negative for myocardial infarction (± peri-infarct ischemia)
    - Consider possibility of hibernating myocardium, need for viability study
  - LV function: EF and wall motion

SELECTED REFERENCES

1. American College of Radiology. ACR-SNMMI-SPR Practice Guideline for the Performance of Cardiac Scintigraphy. http://snmmi.files.cms-plus.com/docs/Cardiac_Scintigraphy_1382731812393_3.pdf. Revised October 1, 2009. Accessed July 18, 2014
2. Struass et al. SNM Procedure Guideline for Myocardial Perfusion Imaging 3.3. http://snmmi.files.cms-plus.com/docs/Myocardial20Perfusion20Imaging203.3.pdf. June 14, 2008. Accessed July 18, 2014
3. Dorbala S et al: SNMMI/ASNC/SCCT guideline for cardiac SPECT/CT and PET/CT 1.0. J Nucl Med. 54(8):1485-507, 2013

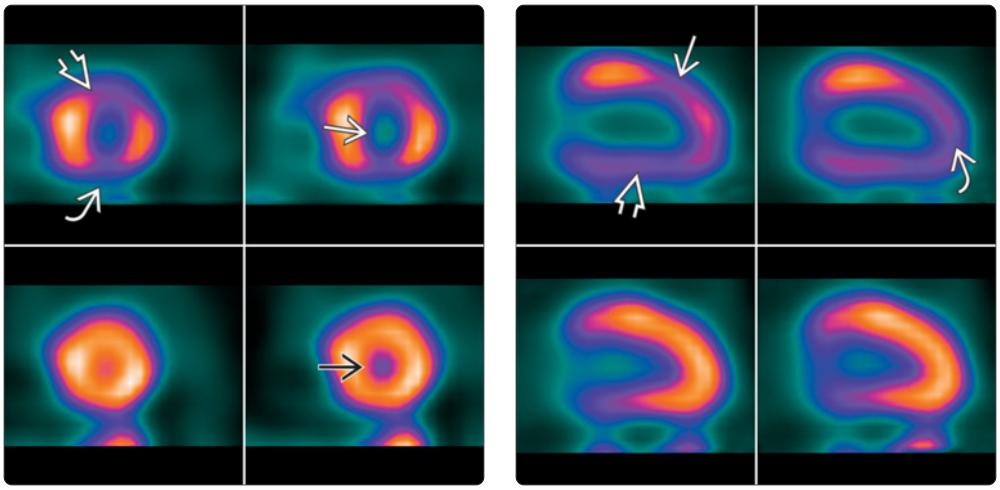

(Left) *Short axis MPI shows transient ischemic dilatation. Note normal endocardial border on rest, which appears to enlarge on stress. This high-risk finding is due to reversible subendocardial ischemia and suggests multivessel disease. Note also the anterior and inferior perfusion defects at stress.* **(Right)** *Vertical long axis MPI views (same patient) show enlarged endocardial border and severe stress-induced perfusion defects involving the anterior wall, inferior wall, and apex. Resting images below are normal.*

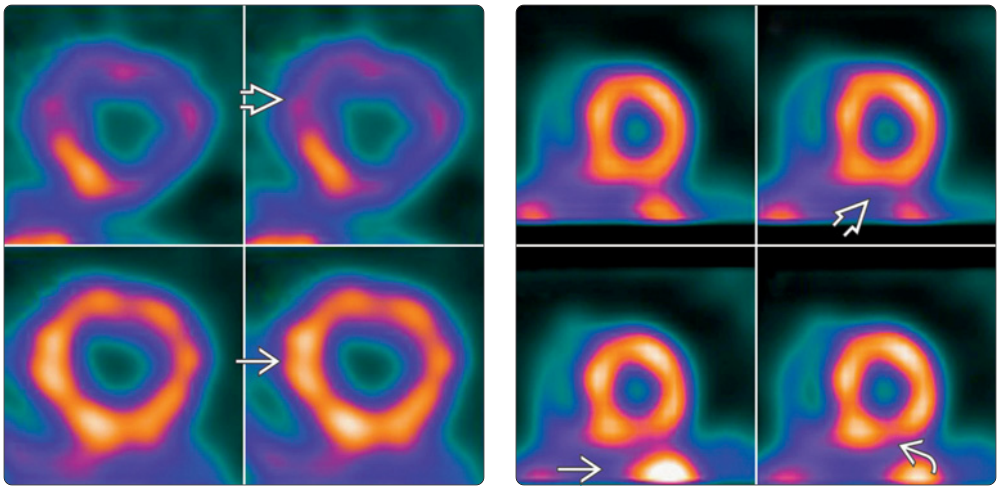

(Left) *Short axis MPI views in an obese patient show heterogeneous myocardium due to poor counts. The top row is prior to CT attenuation correction. The bottom row is after CT attenuation correction.* **(Right)** *Short axis MPI shows high activity in adjacent bowel. Note the adjacent inferior wall shows decreased counts on rest and normal counts on stress. The bowel activity caused decreased counts in the inferior wall due to reconstruction artifact.*

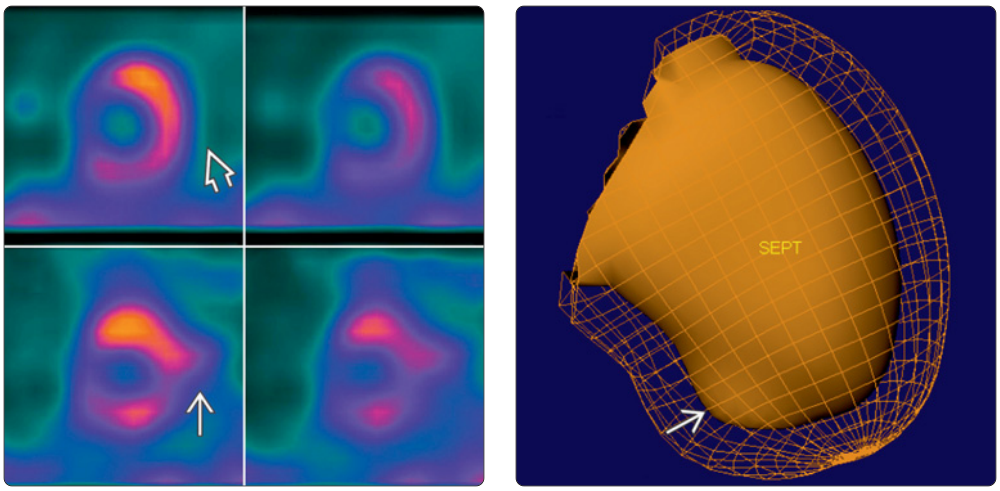

(Left) *Short axis MPI shows extracardiac activity extending from the left ventricle due to patient motion, called the hurricane sign. With motion correction, the hurricane sign disappeared.* **(Right)** *3D MPI rendering of the left ventricle at end systole shows a dilated left ventricle with dyskinesis at the inferoseptum, an apical aneurysm.*

(Left) *Short axis MPI shows multivessel coronary disease. Anteroseptal ⇨ and inferolateral ⇨ perfusion defects are more evident on stress compared with rest images.* **(Right)** *Horizontal long axis MPI in the same patient shows lateral inducible ischemia ⇨.*

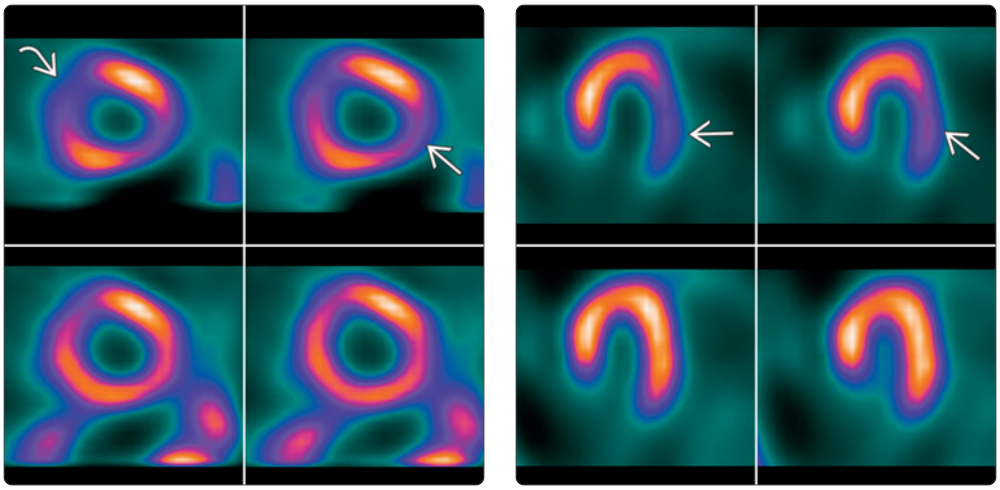

(Left) *Short axis MPI bull's-eye computer analysis in the same patient shows multivessel inducible ischemia in the anteroseptum ⇨, apical ⇨, and inferolateral ⇨ walls on stress imaging.* **(Right)** *Short axis MPI bull's-eye computer analysis in the same patient at rest shows virtually normal perfusion.*

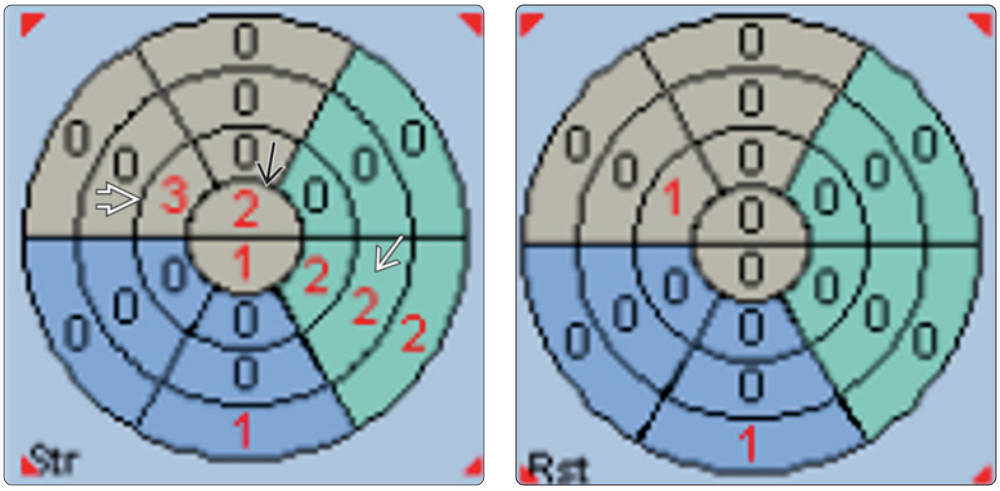

(Left) *3D view of MPI raw images shows normal myocardial radiotracer uptake ⇨.* **(Right)** *3D view of MPI raw images in the same patient who presented for follow-up MPI shows normal myocardial uptake and a large photopenic defect ⇨ surrounding the heart, a pericardial effusion.*

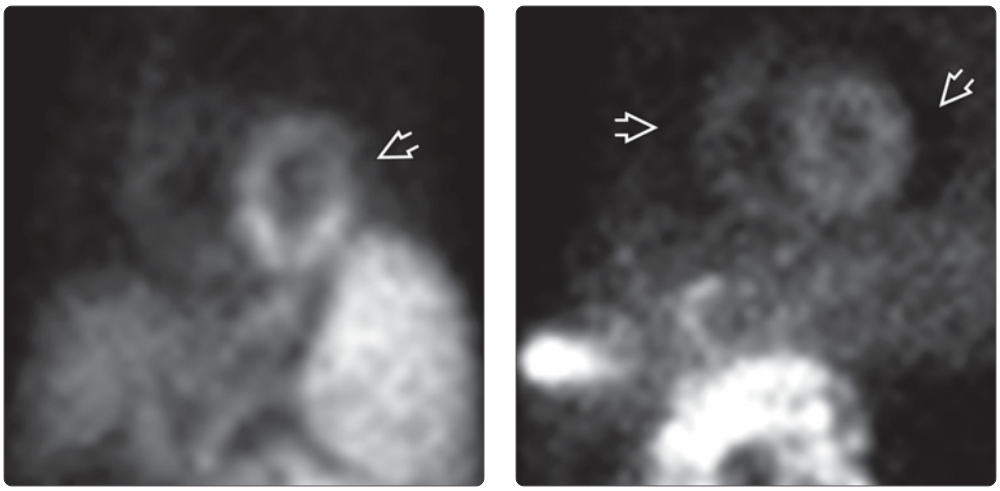

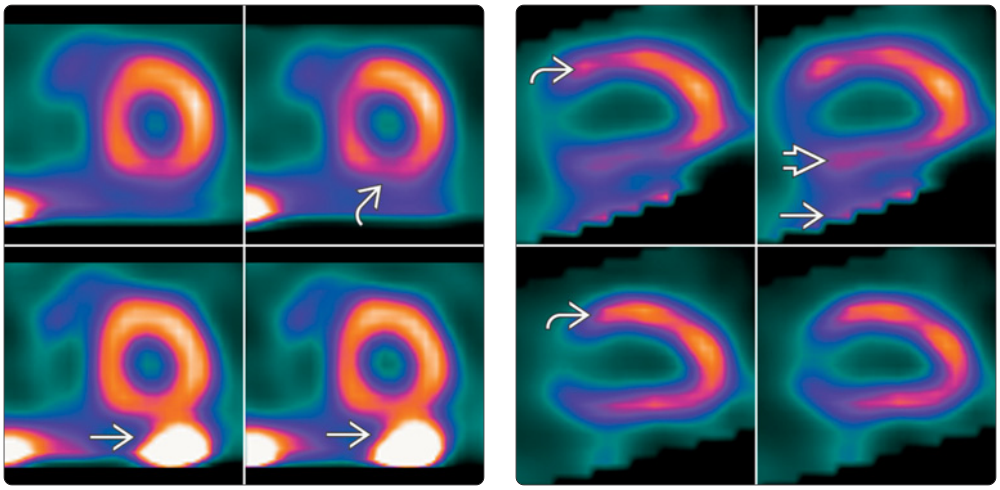

(Left) *Short axis MPI shows high counts in the bowel due to normal radiotracer excretion. Note the relatively diminished perfusion in the inferior wall on repeat image, confirming artifactual scatter of counts into the inferior wall.* **(Right)** *Vertical long axis MPI shows anterior inducible ischemia. Note high counts in bowel on stress images (hidden by computer processing). Coronary artery catheterization showed no inferior wall disease, suggesting reconstruction artifact reduced counts in this area on stress images.*

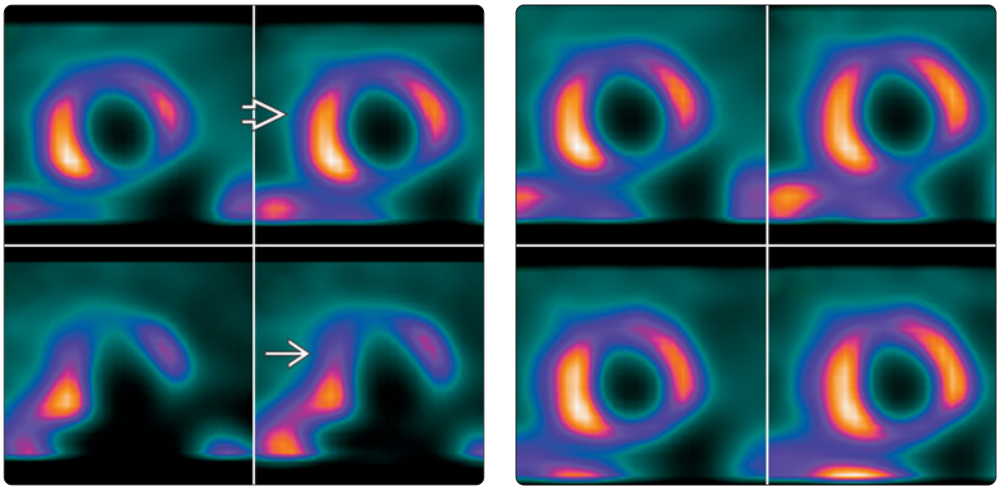

(Left) *Short axis MPI shows decreased counts in the left ventricle on stress that appear to improve on rest.* **(Right)** *Short axis MPI in the same patient with arms up during both rest and stress acquisitions show similar perfusion patterns. Note that the images must be obtained with similar patient positioning to avoid introduction of artifacts.*

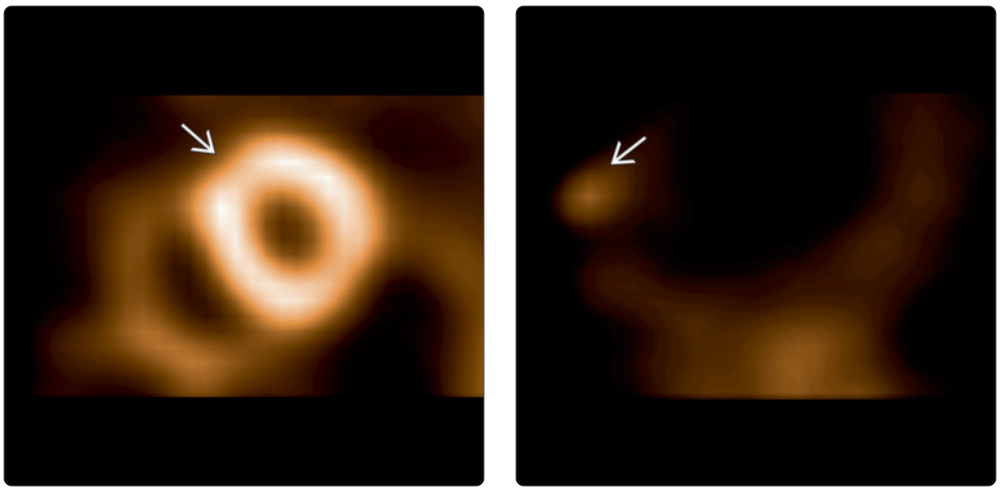

(Left) *Sagittal MPI raw images in an 86-year-old woman with atypical chest pain show normal myocardial uptake.* **(Right)** *Sagittal MPI raw images in the same patient show abnormal uptake in the left breast, a possible breast cancer. Mammographic correlation is necessary for this finding.*

KEY FACTS

TERMINOLOGY

- Myocardial viability evaluation
  - Detection of myocardial hibernation or stunning vs. necrosis/infarction in patients with ischemic cardiomyopathy

IMAGING

- Tc-99m/Tl-201 myocardial perfusion scintigraphy
  - Viability present in 25% of regions called infarction
  - Viability present in up to 50% of patients with infarcted segments
- Perfusion-PET mismatch
  - Myocardial uptake of radioactive glucose analog compared with myocardial uptake of perfusion radiotracer (Tc-99m perfusion agent or Tl-201)
  - Anaerobic glucose utilization in underperfused myocardium = viability
- Tl-201 SPECT viability
  - Rest-redistribution mismatch
  - Delayed myocardial uptake in regions of underperfused myocardium = viability

TOP DIFFERENTIAL DIAGNOSES

- Myocardial hibernation
  - Chronic myocardial dysfunction due to chronically decreased myocardial perfusion (chronic total occlusions)
  - Regions of abnormal perfusion will show F-18 FDG utilization or redistribution on Tl-201
- Myocardial stunning
  - Temporary myocardial dysfunction due to short-term underperfusion or lack of perfusion to myocardium
  - Regions of abnormal perfusion will show F-18 FDG utilization or redistribution on Tl-201
- Myocardial infarction
  - Myocardial necrosis and remodeling (scar)
  - Regions of abnormal perfusion will show lack of F-18 FDG utilization or lack of redistribution on Tl-201

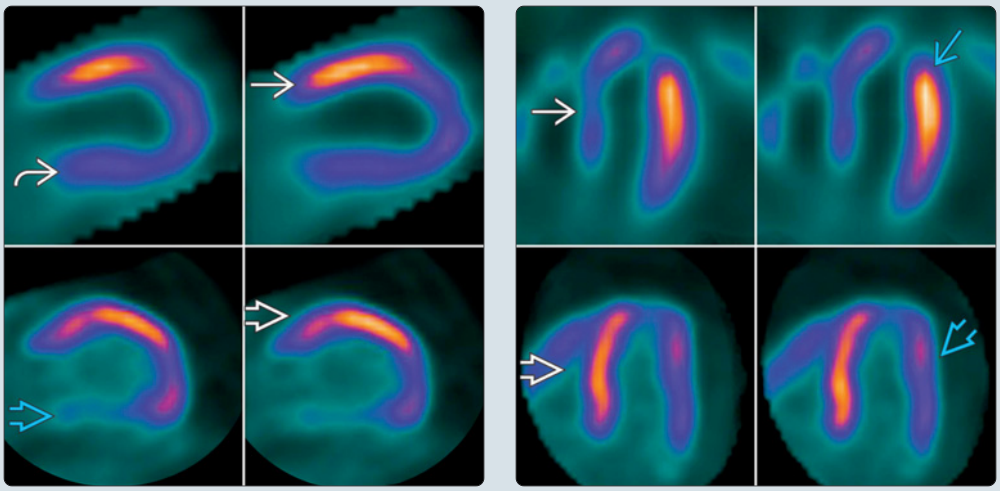

(Left) *Vertical long axis F-18 FDG PET viability shows normal perfusion in the anterior wall ➡ with associated glucose metabolism ➡. This confirms glucose is an available substrate for hypoperfused inferior wall ➡, which does not show viability on PET ➡.* **(Right)** *Horizontal long axis F-18 FDG PET viability shows hypoperfused septum ➡ with glucose utilization ➡, signifying viability. Note that the normally perfused lateral wall ➡ is not utilizing glucose ➡, signifying free fatty acids are being utilized.*

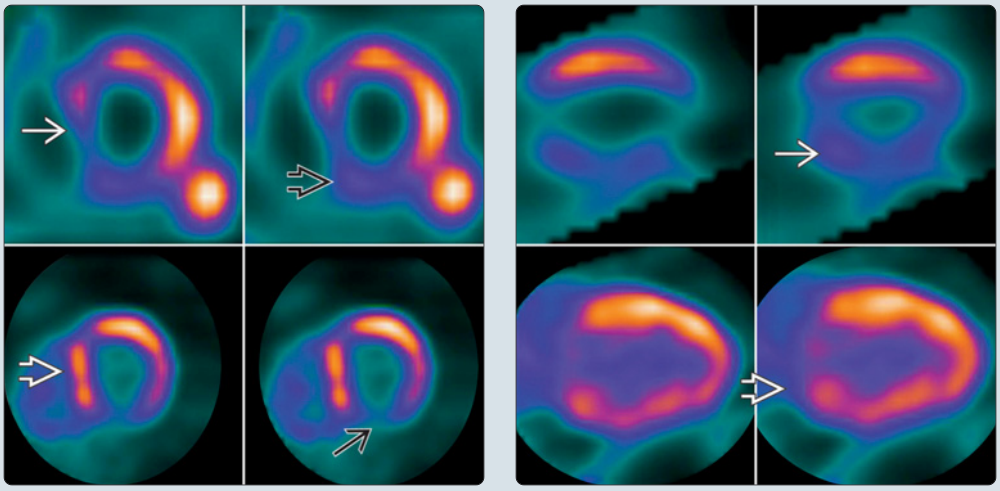

(Left) *Short axis F-18 FDG PET viability shows hypoperfused septum ➡ that is utilizing glucose ➡, signifying viability. Note the inferior myocardial infarction ➡ that is not viable ➡.* **(Right)** *Vertical long axis F-18 FDG PET viability shows inferior wall perfusion ➡ and glucose metabolism ➡ mismatch. This suggests that the inferior wall will improve in contractility after revascularization.*